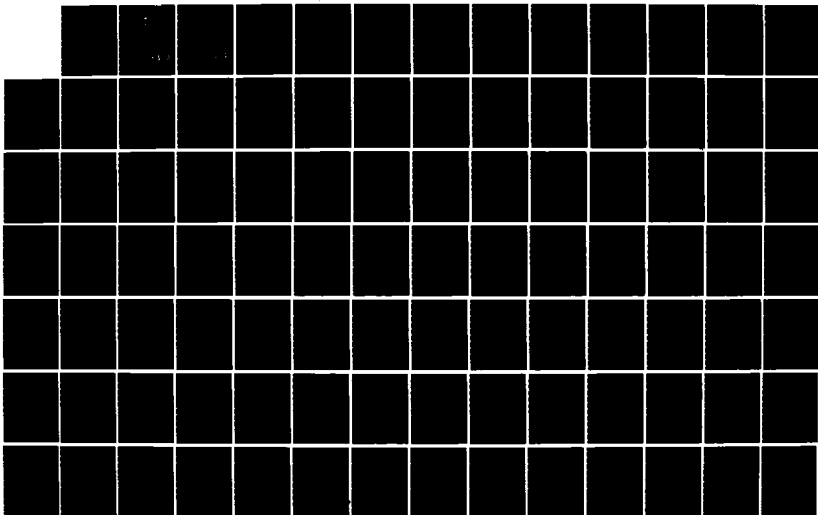
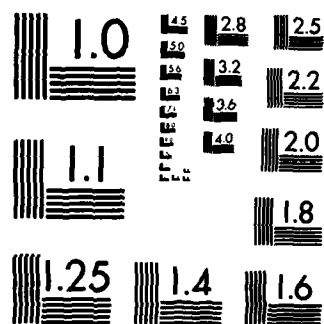


AD-A151 710 MARGIN LEVELING ALGORITHM FOR FULLY SATURATED SATELLITE 1/2
TRANSPONDER WITH..(U) AIR FORCE INST OF TECH
WRIGHT-PATTERSON AFB OH SCHOOL OF ENGI.. E J PUTT
UNCLASSIFIED DEC 84 AFIT/GE/ENG/84D-52 F/G 17/2 NL





MICROCOPY RESOLUTION TEST CHART
NATIONAL BUREAU OF STANDARDS-1963-A

AD-A151 710

DTIC
①



MARGIN LEVELING ALGORITHM FOR FULLY SATURATED
SATELLITE TRANSPONDER WITH CDMA SIGNALLING

THESIS

Edward J. Putt
Second Lieutenant, USAF

AFIT/GE/ENG/84D-52

DISTRIBUTION STATEMENT A

Approved for public release
Distribution Unlimited

DEPARTMENT OF THE AIR FORCE
AIR UNIVERSITY

AIR FORCE INSTITUTE OF TECHNOLOGY

Wright-Patterson Air Force Base, Ohio

85 03 13 131

REPRODUCED AT GOVERNMENT EXPENSE

DTIC FILE COPY

DTIC
ELECTE
MAR 28 1985
S B D

AFIT/GE/ENG/84D-52

MARGIN LEVELING ALGORITHM FOR FULLY SATURATED
SATELLITE TRANSPONDER WITH CDMA SIGNALLING

THESIS

Edward J. Putt
Second Lieutenant, USAF

AFIT/GE/ENG/84D-52

DTIC
ELECTE
MAR 28 1985
S B D

Approved for public release; distribution unlimited

AFIT/GE/ENG/84D-52

MARGIN LEVELING ALGORITHM FOR FULLY SATURATED
SATELLITE TRANSPONDER WITH CDMA SIGNALLING

THESIS

Presented to the Faculty of the School of Engineering
of the Air Force Institute of Technology
Air University
In Partial Fulfillment of the
Requirements for the Degree of
Master of Science in Electrical Engineering

Edward J. Putt, B.S.

Second Lieutenant, USAF

December 1984

Approved for public release; distribution unlimited

Preface

The purpose of this study was to develop a margin leveling algorithm for a fully saturated satellite transponder where code division multiple access communications was used as the signalling scheme. The algorithm successfully performed margin leveling on up to twenty links. The leveling of additional links was not feasible due to the limited computer time available at AFIT.

At this point I would like to thank those who have assisted and advised me during the work on this thesis. I greatly appreciate the efforts of my thesis advisor, Maj Kenneth G. Castor, who provided assistance and encouragement in times of need. I would also like to thank Lawrence W. Krebs of the Defense Communications Engineering Center for his expertise in the area of satellite communications as well as his enlightening telephone conversation. Finally, I wish to thank my wife Nora for her proof reading efforts and also for her additional patience.

Edward J. Putt



Accession For	
NTIS CPARI	<input checked="checked" type="checkbox"/>
DTIC TAB	<input type="checkbox"/>
Unannounced	<input type="checkbox"/>
Justification	
Distribution/	
Availability Codes	
Dist	Avail and/or Special
A-1	

Table of Contents

	Page
Preface	11
List of Figures	v
List of Tables	vii
Abstract	viii
I. Introduction	1
II. Satellite Communications Theory	4
Link Equations	4
Satellite Transponder Model	11
Band Pass Limiter	12
Travelling Wave Tube Amplifier	18
Introduction to CDMA	24
III. Hard Limiting of Multiple Carriers	28
CDMA Link Analysis with Linear Transponder	28
Analysis of Hard Limited CDMA Signals	31
IV. Verification of Preliminary Results	42
Two Link Verification	42
Four Link Verification	44
V. Margin Leveling Algorithm	47
Margin Leveling Scenarios	47
Margin Leveling Algorithm	48
VI. Performance and Results of Margin Leveling Algorithm	57
Margin Leveling Results	57
CPU Time Constraints	60

	Page
VII. Recommendations and Conclusions	72
Integration Speed	72
Additional Recommendations for Decreasing CPU Time ...	73
Further Study	74
Conclusions	75
Appendix A: Correlation Analysis of Nonlinear Devices	77
Single Carrier Correlation Analysis	77
Multiple Carrier Correlation Analysis	81
Bibliography	86
Vita	87

List of Figures

Figure	Page
2.1. Ideal Uplink-downlink Satellite Model	8
2.2. Satellite Transponder Model	11
2.3. Limiter Input-Output Characteristic	12
2.4. Γ Versus Uplink Carrier-to-Noise Ratio	17
2.5. TWTA AM/AM Conversion Characteristic Curve	19
2.6. TWTA AM/PM Conversion Characteristic Curve	21
2.7. Γ' , Γ^2 Versus Uplink Carrier-to-Noise Ratio	23
2.8. Direct Sequence CDMA Modulator/Transmitter	25
2.9. Direct Sequence CDMA Demodulator/Receiver	26
3.1. Multiple Satellite Channel Model	29
4.1. BPL Output Power Ratio vs. Input Power Ratio (2 Links) ...	43
4.2. TWTA Output Power Ratio vs. BPL Input Power Ratio (2 Links)	44
4.3. BPL Output Power vs. Input Power Ratio (4 Links)	45
4.4. BPL Signal Suppression vs. Input Power Ratio (4 Links) ...	46
5.1a Margin Leveling Algorithm (Convergence Routine)	49
5.1b Margin Leveling Algorithm (Leveling Routine)	50
5.2. Illustration of Margin Leveling Progression	54
6.1. CPU Time Versus Number of Links, Option 0	63
6.2. CPU Time Versus Number of Links, Option 1, 1 db leveling .	64
6.3. CPU Time Versus Number of Links, Option 1, 2 db leveling .	65
6.4. CPU Time Versus Number of Links, Option 1, 4 db leveling .	66

Figure	Page
6.5. CPU Time Versus Number of Links, Option 1, 6 db leveling .	67
6.6. CPU Time Versus Number of Links, Option 1, 10 db leveling	68
6.7. CPU Time Versus Number of Links (Logrithmic), Option 0, ..	69
6.8. CPU Time Versus Number of Links (Logrithmic), Option 1, 10 db leveling...	70

List of Tables

Table	Page
5.1. Margin Leveling Results of a Two Link System, Option 0 Selected	56
5.2. Margin Leveling Results of a Two Link System, Option 1 Selected	56
6.1. Margin Leveling Results for Nonhomogeneous 16 Link System, Option 0	58
6.2. Margin Leveling Results for Nonhomogeneous 16 Link System, Option 1	58
6.3. Link Configuration for 16 Link Nonhomogeneous System	59
6.4. Link Configuration Used to Evaluate Required CPU Time vs. Number of Links	61
6.5. Specific Link Configurations with Respect to the Number of Links	62
6.6. Predicted CPU Time to Perform Margin Leveling (CYBER Computer)	71

Abstract

↪ For satellite communications in a noninterfering environment, a specific downlink carrier-to-noise ratio ^(CNR) is needed to achieve a desired bit error rate. In an interfering environment, an additional ^{C/N₀} carrier-to-noise ratio or margin is needed to overcome ~~the~~ interfering effects. A situation may arise where the desired margins cannot be achieved due to limited uplink and satellite transmit power. If this is the case, margin leveling should occur in order to decrease the desired margins in a specific manner until all margins are achieved.

The goal of this thesis is to develop a margin leveling algorithm under specific constraints. The satellite under study is assumed to be operating with the ^{Traveling wave tube amplifier} TWA in full saturation. The signalling scheme used is direct sequence code division multiple access ^(CDMA) communications.

Two methods of margin leveling are created. The first being the margin leveling of only the links in which the desired margins are not achieved, The second being the margin leveling of all links whether the desired margins are achieved or not. In the latter case, all links are leveled by an equal amount.

Due to the specific satellite model used, the cascade of two bandpass limiters, the amount of computer time needed to perform margin leveling is quite high. It is found that the computer time needed to perform margin leveling increases proportionally to the square of the number of links accessing the satellite.

Given the proper amount of computer time, the results of the margin leveling algorithm were as expected. For either case of margin

leveling, the algorithm produced leveled margins with the difference between the desired and the leveled margins being a minimum.

MARGIN LEVELING ALGORITHM FOR FULLY SATURATED SATELLITE TRANSPONDER WITH CDMA SIGNALLING

I. Introduction

In digital satellite communications, the desired quality of service, specified by a bit error rate, is obtained by achieving specific downlink carrier-to-noise ratios. To overcome the transient effects of rain attenuation and atmospheric scintillation which may degrade the received signal, each link is provided an additional amount of signal power which in turn creates a "margin" for the downlink carrier-to-noise ratio.

The goal of this thesis is to develop an algorithm which will calculate the uplink powers required to provide each link its desired margin. If one or more of the desired margins are unachievable due to limited uplink power, then one of two scenarios shall occur. Either the margin for all links shall be reduced (leveled) by an equal amount until all margins are achieved or only the unachievable margins shall be reduced until all margins are achieved. In either case, the difference between the desired margin and the leveled margin must be a minimum, i.e. at least one uplink power will be maximized.

The problem becomes difficult when this goal is sought amidst an environment of non-homogeneous earth terminal antennas ranging from 6 to 60 feet in diameter and with non-uniform margin allocations. Due to the power sharing in the satellite transponder, it is impossible to

the output signal power can be simplified to give

$$P_{so} = (V_1^2 A^2 / \pi R_n(0)) e^{-A^2 / 2 R_n(0)} [I_0(A^2 / 4 R_n(0)) + (I_1(A^2 / 4 R_n(0)))^2] \quad (2.33)$$

The output signal power can now be expressed in terms of the uplink carrier-to-noise ratio where $A^2/2$ is equivalent to the uplink signal power entering the BPL, $g_1^P L_u$, and $R_n(0)$ is equivalent to the uplink noise power entering the BPL, $g_1^P P_{nu}$. With these substitutions and the fact that

$$CNR_u = g_1^P L_u / g_1^P P_{nu} = P_{su} L_u / P_{nu} \quad (2.34)$$

the output signal power is given as

$$P_{so} = (2V_1^2 / \pi) CNR_u e^{-CNR_u} [I_0(CNR_u / 2) + I_1(CNR_u / 2)]^2 \quad (2.35)$$

From this equation, it looks as though the output signal power is independent of the LNA gain, g_1 . This is not entirely true since the gain does effect the noise power via the noise figure, F . A larger gain provides a lower system noise figure which in turn decreases the total noise power.

To find an expression for the carrier-to-noise ratio out of the BPL, the output noise power is required. Since the total output of the BPL is made up of the signal power plus noise power, the output noise power, P_{no} , can be written as the difference between the total power and the signal power.

$$P_{no} = P_o - P_{so} \quad (2.36)$$

The resulting output carrier-to-noise ratio, CNR_{BPL} , can be

where

A = amplitude of input phase modulation entering BPL

$R_n(0)$ = noise power entering BPL

$G(\omega)$ = Fourier Transform of limiter input-output characteristic

For the hard limiter, the fourier transform of $g(x)$ is given by

$$G(\omega) = F(g(x)) = 2V_1/j\omega \quad (2.28)$$

Substituting Eq (2.28) into Eq (2.27) gives

$$P_{so} = 2[(2\pi)^{-1} \int_{-\infty}^{\infty} (2V_1/\omega) J_1(\omega A) e^{-R_n(0)\omega^2/2} d\omega]^2 \quad (2.29)$$

Since $J_1(\omega A)$ is an odd function with respect to ω (3:94), the function, $[(J_1(\omega A) \exp(-R_n(0)\omega^2/2))/\omega]$, is even with respect to ω .

With this knowledge, the output signal power can be written as

$$P_{so} = 2[(2/\pi) \int_0^{\infty} (V_1/\omega) J_1(\omega A) e^{-R_n(0)\omega^2/2} d\omega]^2 \quad (2.30)$$

This integral can be evaluated (2:1079) to give

$$P_{so} = 2 \left[\frac{AV_1 \Gamma(\frac{1}{2}) {}_1F_1(\frac{1}{2}, 2, -a^2/2R_n(0))}{2\pi(R_n(0)/2)^{\frac{1}{2}} \Gamma(2)} \right]^2 \quad (2.31)$$

where ${}_1F_1(a, b, x)$ is the confluent hypergeometric function and $\Gamma(x)$ is the gamma function. Eq (2.31) can be further simplified since

$\Gamma(\frac{1}{2}) = (\pi)^{\frac{1}{2}}$ and $\Gamma(2) = 1$. With the use of the following identity (2:1076)

$${}_1F_1(\frac{1}{2}, 2, -x) = e^{-x/2} [I_0(x/2) + I_1(x/2)] \quad (2.32)$$

$$g(x) = V_1(u(x) - u(-x)) \quad (2.23)$$

For a combined carrier and noise input of the form

$$x(t) = g_1 a(t) \cos(\omega_c t + \theta(t)) \quad (2.24)$$

with $a(t)$ and $\theta(t)$ both being random variables, the limiter output will consist of a square wave of amplitude V_1 having identical phase and frequency to that of the input.

From fourier series analysis, the BPL output will yield

$$y(t) = (4V_1/\pi) \cos(\omega_c t + \theta(t)) \quad (2.25)$$

Therefore, the BPL produces an rf carrier output with the same frequency and phase as that of the input but with a constant amplitude independent of the input amplitude. Thus, the BPL eliminates amplitude modulation while preserving phase modulation.

The total output power, P_o , consisting of carrier and noise power is now given as

$$P_o = (4V_1/\pi)^2/2 = 8V_1^2/\pi^2 \quad (2.26)$$

For a phase modulated input plus narrow band gaussian noise, the output signal power, P_{so} , has been shown in appendix A, Eq (A.21), to be

$$P_{so} = 2[(2\pi)^{-1} \int_{-\infty}^{\infty} G(\omega) j J_1(\omega A) e^{-R_n(0)\omega^2/2} d\omega]^2 \quad (2.27)$$

minimal effect on the uplink carrier-to-noise ratio and is not included in the downlink carrier-to-noise ratio analysis. The remaining stages consisting of the band pass limiter (BPL) and the travelling wave tube amplifier (TWTA) have significant effect on the uplink carrier-to-noise ratio and are included in the downlink analysis. The band pass limiter is analyzed first.

Band Pass Limiter. The limiter is modeled as a hard limiter having the input-output characteristics as shown in figure 2.3. A hard limiter is typically used prior to the TWTA to assure a constant

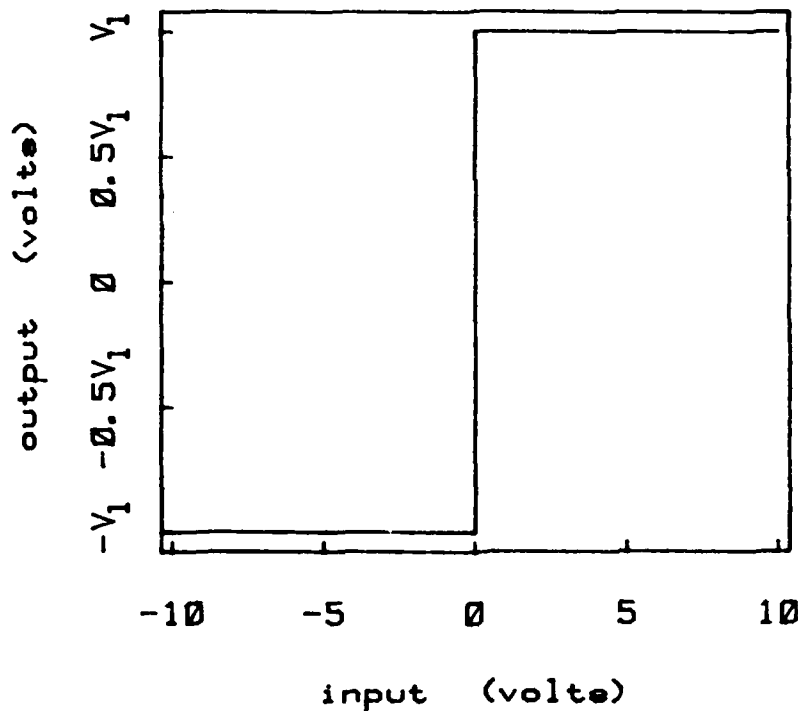


Fig. 2.3. Limiter Input-Output Characteristic

envelope input into the TWTA. The input-output characteristic, $g(x)$, can also be written in terms of unit step functions, $u(x)$.

$$\text{CNR} = E_b/N_o + R_d - B_{\text{rf}} + M \quad (\text{db}) \quad (2.22)$$

where M is the link margin.

Satellite Transponder Model

A basic model of a satellite transponder is shown in figure 2.2. The received signals enter the satellite through the antenna and the

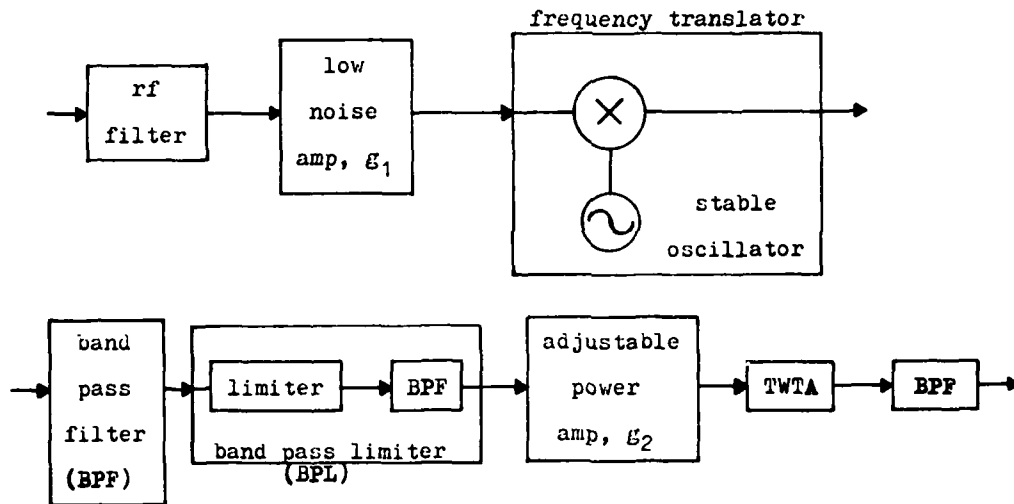


Fig. 2.2. Satellite Transponder Model

low noise rf front end. The noise figure of the rf front end contributes to the uplink noise power as shown in Eqs (2.8) and (2.9). The frequency translator shifts the uplink spectrum from one frequency band to a another non-overlapping band and has minimal affect on the carrier and noise powers. Thus, the translator has a

E_b/N_o is used to characterize the performance of a system. E_b/N_o is the energy per bit (E_b) divided by the noise spectral level (N_o). The downlink carrier-to-noise ratio can be written as a function of E_b/N_o as shown here.

$$\text{CNR} = \text{Carrier Power} / \text{Noise Power} \quad (2.20)$$

From the relationship between power and energy and Eq (2.8), the carrier-to-noise ratio can be rewritten as

$$\text{CNR} = E_b / T_b N_o B_{\text{rf}} = E_b R_d / N_o B_{\text{rf}} \quad (2.21)$$

where

$$\begin{aligned} E_b &= \text{energy per bit} \\ T_b &= \text{bit duration} = 1/\text{data rate} = 1/R_d \\ B_{\text{rf}} &= \text{rf bandwidth} \end{aligned}$$

Given a desirable probability of bit error and the type of signalling (i.e. PSK, FSK, ...) it is possible to find the E_b/N_o needed to provide that probability of bit error. With this E_b/N_o , the data rate, and the rf bandwidth, the required downlink carrier-to-noise ratio can then be found.

It is common practice to include a link margin in the calculations of the desired carrier-to-noise ratio. The margin is provided to overcome the transient effects of rain attenuation and atmospheric scintillation which may degrade the received signal. In a jamming environment, the margin may be added to defeat the jammer. For either case the downlink carrier-to-noise ratio can now be written as

loss, L_d , is defined as

$$L_d = g_{2s} L_{pd} L_{ad} g_{lr} \quad (2.14)$$

From Eqs (2.12) and (2.13), the total received power is then

$$P_{rd} = GP_{nu} L_d + P_{nd} + GP_{su} L_u L_d \quad (2.15)$$

The downlink carrier-to-noise ratio (CNR_d) at the receiver can then be written as

$$CNR_d = \frac{\text{received signal power}}{\text{total received noise power}} = \frac{GP_{su} L_u L_d}{GP_{nu} L_d + P_{nd}} \quad (2.16)$$

If the uplink carrier-to-noise ratio is defined as

$$CNR_u = \frac{\text{received signal power at satellite}}{\text{received noise power at satellite}} = \frac{P_{su} L_u}{P_{nu}} \quad (2.17)$$

and the receiver carrier-to-noise ratio is defined as

$$CNR_r = \frac{\text{received signal power at receiver}}{\text{received downlink noise power at receiver}} = \frac{P_{su} G L_u L_d}{P_{nd}} \quad (2.18)$$

From Eqs (2.16), (2.17) and (2.18), the downlink CNR can now be written as

$$CNR_d^{-1} = CNR_u^{-1} + CNR_r^{-1} \quad (2.19)$$

It is seen that the downlink carrier-to-noise ratio depends upon the uplink carrier-to-noise ratio as well as the receiver carrier-to-noise ratio and it can never exceed either one.

For digital communications, a commonly used parameter known as

where

- P_{ru} = total uplink power collected at satellite front end
- P_{nu} = total uplink noise power collected at satellite front end
- P_{su} = uplink power transmitted
- L_u = uplink gains and losses = $(g_{1t} L_{au} L_{pu} g_{1s})$

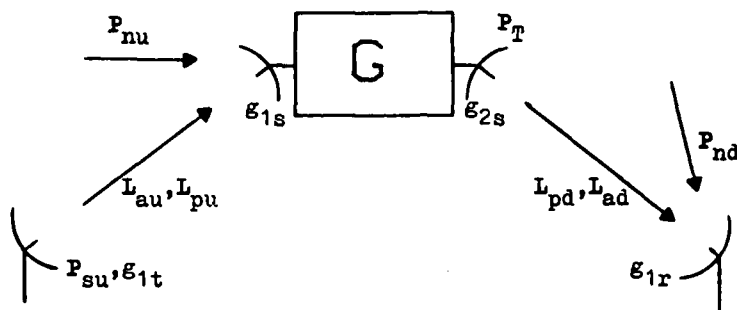


Fig. 2.1. Ideal Uplink-Downlink Satellite Model

With a gain of G , the transmitted power prior to the satellite transmitting antenna, P_T , is then

$$P_T = GP_{nu} + GP_{su} L_u \quad (2.12)$$

The total received power at the downlink receiver, P_{rd} , is a combination of downlink noise and transmitted satellite power and is written as

$$P_{rd} = P_T L_d + P_{nd} \quad (2.13)$$

where P_{nd} is the total received downlink noise power and the downlink

directed at the earth, the value of T_b is a fairly constant 300 °K. However, for an earth based antenna directed into space, the value of T_b depends on the transmitted frequency, the elevation angle and the rainfall rate. Moderate rainstorms below 10 mm/hr have only minimal affect on T_b , but severe rainstorms can cause T_b to increase by as much as 50 °K.

From Eqs (2.4), (2.7) and (2.8), the carrier-to-noise ratio can be written as

$$CNR = EIRP(L_p L_a)(g_r/T_{eq})(1/B_r)(1/k) \quad (2.10)$$

As arranged, the carrier-to-noise ratio is a product of transmitter, propagation, receiver and bandwidth parameters.

It is now possible to perform an up-downlink analysis on a simple, one link, satellite transponder assumed to have linear gain and frequency translation. Frequency translation is the shifting or translating of the uplink spectrum to an adjacent, non-overlapping frequency band. This allows the use of a single antenna for both reception and transmission.

Referring to figure 2.1, the total uplink power collected at the satellite front end consists of a signal and a noise component and can be written as

$$P_{ru} = P_{nu} + P_{su} L_u \quad (2.11)$$

The CNR is defined as

$$\text{CNR} = (P_r / P_n) \quad (2.7)$$

where

$$\begin{aligned} P_r &= \text{signal power received} \\ P_n &= \text{noise power received} \end{aligned}$$

The received noise power is the undesired power which interferes with the desired signal. The main contributor of the noise power is cosmic sources and receiver electronics. The amount of noise power present depends upon the following relationships:

$$P_n = k T_{eq} B_r = N_o B_r \quad (2.8)$$

where

$$\begin{aligned} k &= \text{Boltzman's constant} = 1.379 \times 10^{-23}, \text{ w/}^\circ\text{K Hz} \\ T_{eq} &= \text{equivalent receiver noise temperature, } ^\circ\text{K} \\ B_r &= \text{receiver bandwidth} \end{aligned}$$

The equivalent noise temperature can be written as

$$T_{eq} = T_b + (F-1)T_o \quad (2.9)$$

where

$$\begin{aligned} T_b &= \text{background noise temperature (antenna noise temperature), } ^\circ\text{K} \\ F &= \text{receiver noise figure} \\ T_o &= 290 ^\circ\text{K} \end{aligned}$$

The background noise temperature accounts for noise collected by the antenna and the noise figure accounts for any additional noise. The value of T_b is dependent upon the specific noise characteristics which the antenna is observing. For a satellite receiving antenna

where

P_r = power received
 P_t = power transmitted
 g_t = gain of transmit antenna
 L_a = atmospheric losses

The effective area of the receiving antenna can be written in terms of the receiving antenna gain, g_r , and the wavelength, λ .

$$A_e = \lambda^2 g_r / 4\pi \quad (2.2)$$

Combining Eqs (2.1) and (2.2) gives

$$P_r = P_t g_t (\lambda / 4\pi r)^2 L_a g_r \quad (2.3)$$

which can be rewritten as

$$P_r = (EIRP) L_p L_a g_r \quad (2.4)$$

where EIRP is the effective isotropic radiated power from the transmitter, $(P_t g_t)$, and L_p is defined as

$$L_p = (\lambda / 4\pi r)^2 \quad (2.5)$$

The parameter L_p is known as an effective propagation loss due to the spreading of the signal as it propagates away from the source. Eq (2.4) can also be written as

$$P_r = EIRP + L_p + L_a + g_r \quad (\text{db}) \quad (2.6)$$

A key parameter characterizing the performance of a communications system is the received carrier-to-noise ratio (CNR).

II. Satellite Communications Theory

The goal of this thesis is to create an algorithm that levels the margins of various satellite links given that the satellite transponder is operating in saturation and code division multiple access (CDMA) communications is used for each link. In order to fully understand the problem, it is essential that the basic satellite channel be understood first.

This chapter presents some of the basic theory behind communication satellites. The satellite channel is reviewed and the basic satellite link equations are derived. The satellite transponder is also discussed and near the end of this chapter code division multiple access (CDMA) communications is introduced.

Link Equations

The theory presented in this and the upcoming section is referenced from Gagliardi (1:83-192).

On an earth to satellite communications link there exists an earth transmitter and a satellite receiver separated by a propagation distance r . For a transmit power of P_t , the power intercepted by the satellite receiving antenna with an effective area of A_e , is given by

$$P_r = (P_t g_t A_e L) / (4\pi r^2) \quad (2.1)$$

discusses the two types of margin leveling to be achieved as well as the algorithm used to achieve margin leveling. The results of margin leveling is shown in chapter 6 as well as the time required for the algorithm to converge as the number of link accessing the satellite increases. In chapter 7, limitations to the algorithm are discussed and recommendations are given for algorithm improvement.

create a change in the carrier-to-noise ratio of a single link without effecting the carrier-to-noise ratios of the other links. This problem becomes more severe when the satellite transponder is saturated as would be the case when trying to prevent the AM-PM effects which occur in a non-saturated transponder. The effect of the saturated transponder is to cause signals with low input carrier-to-noise ratios to become even lower at the output and to cause signals with high input carrier-to-noise ratios to become higher at the output.

To deal with these problems, a mathematical model of the saturated satellite transponder is created and analyzed to determine the downlink carrier-to-noise ratio given the uplink, the downlink, and the satellite parameters. The resulting equations which emerge are analytically noninvertible, so successive iteration of the derived equations is performed until the desired margins for each link are either achieved or the uplink power for that link is maximized. At this point, margin leveling is performed if necessary.

Chapter 2 of this report deals with the basic theory of satellite communications involving link equations, effects of a hard limiting and an introduction to code division multiple access communications. Chapter 3 discusses the specific satellite model used as well as the derivation of the equations which obtain the downlink carrier-to-noise ratio for the satellite links.

Chapter 4 discusses the validity of the downlink carrier-to-noise ratio equations by comparing intermediate results with the known results of other authors given a 2 and 4 link system. Chapter 5

written as

$$\text{CNR}_{\text{BPL}} = P_{\text{so}}/P_{\text{no}} = P_{\text{so}}/(P_{\text{o}} - P_{\text{so}}) = (P_{\text{so}}/P_{\text{o}})/(1 - P_{\text{so}}/P_{\text{o}}) \quad (2.37)$$

From Eqs (2.26) and (2.35), $P_{\text{so}}/P_{\text{o}}$ is shown to be

$$P_{\text{so}}/P_{\text{o}} = (\pi/4)\text{CNR}_{\text{u}} e^{-\text{CNR}_{\text{u}}} [I_0(\text{CNR}_{\text{u}}/2) + I_1(\text{CNR}_{\text{u}}/2)]^2 \quad (2.38)$$

A normalized ratio, Γ , is defined such that

$$\Gamma = \text{CNR}_{\text{BPL}}/\text{CNR}_{\text{u}} \quad (2.39)$$

which can be rewritten as

$$\Gamma = \frac{(\pi/4)e^{-\text{CNR}_{\text{u}}} [I_0(\text{CNR}_{\text{u}}/2) + I_1(\text{CNR}_{\text{u}}/2)]^2}{1 - (\pi/4)\text{CNR}_{\text{u}} e^{-\text{CNR}_{\text{u}}} [I_0(\text{CNR}_{\text{u}}/2) + I_1(\text{CNR}_{\text{u}}/2)]^2} \quad (2.40)$$

A graph of Γ versus CNR_{u} is shown in figure 2.5. This figure shows the effect which the BPL has on the uplink carrier-to-noise ratio. It is seen that the BPL causes an increase in the uplink carrier-to-noise ratio for large input ratios but causes a slight degradation in the uplink carrier-to-noise ratio when the input ratio is low.

From Eq (2.19), the downlink carrier-to-noise ratio can now be written as

$$\text{CNR}_{\text{d}}^{-1} = (\Gamma \text{CNR}_{\text{u}})^{-1} + \text{CNR}^{-1} \quad (2.41)$$

where Γ accounts for the effects of the BPL.

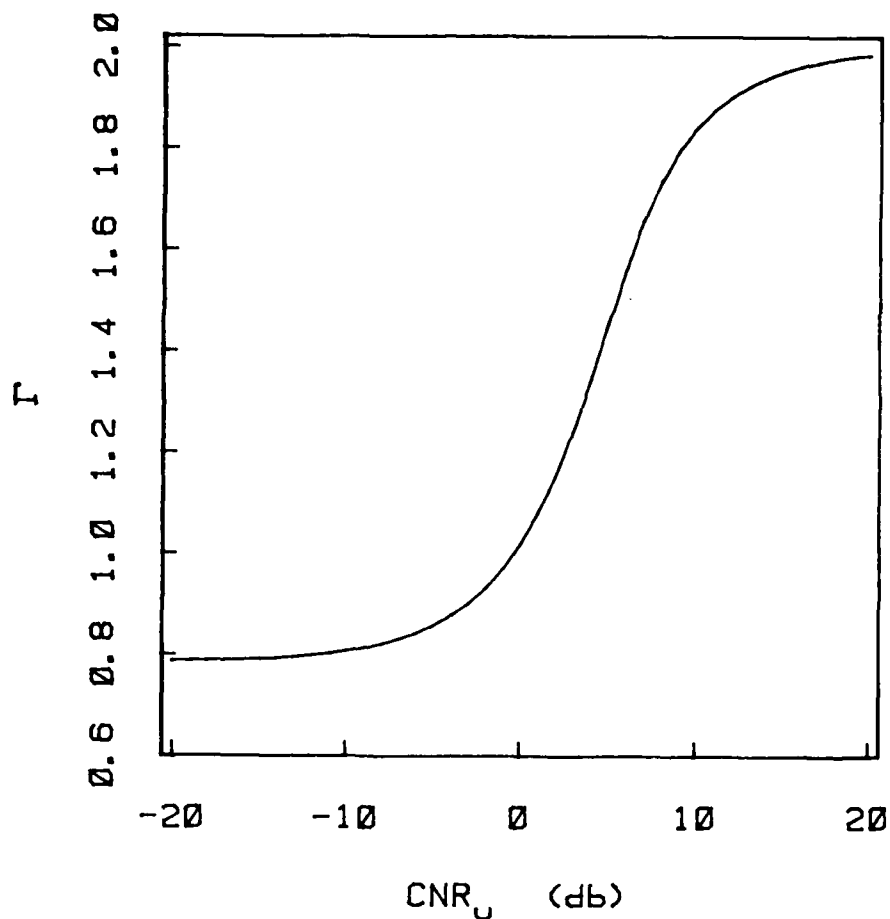


Fig. 2.4. Γ Versus Uplink Carrier-to-Noise Ratio

From Eq (2.41), it appears that the receiver carrier-to-noise ratio is unaffected. However, this is misleading as can be seen by the definition of the receiver carrier-to-noise ratio.

From Eq (2.18), the receiver carrier-to-noise ratio is defined as

$$CNR_r = \frac{\text{signal power at receiver}}{\text{downlink noise power at receiver}} \quad (2.42)$$

which for the case of the BPL preceeding a TWTA with a linear gain of

G, is written as

$$\text{CNR}_r = P_{so} G_L / P_{nd} = f(\text{CNR}_u, P_{nd}) \quad (2.43)$$

The receiver carrier-to-noise ratio is no longer just a function of the uplink signal power and downlink noise power as shown in Eq (2.18). The receiver carrier-to-noise ratio is also a function of the uplink carrier-to-noise ratio since P_{so} is a function of the uplink carrier-to-noise ratio.

Travelling Wave Tube Amplifier. Following the bandpass limiter in the satellite model is the adjustable power amplifier and the travelling wave tube amplifier (TWTA) which are used for final amplification of the communication signals prior to retransmission.

The TWTA is designed to amplify constant amplitude, phase-modulated signals. Variations of input signal amplitude during amplification produce undesirable phase and amplitude modulation of the input signal, thus the need for a limiter prior to the TWTA. The undesirable phase modulation is referred to as AM/PM conversion while the undesirable amplitude modulation is referred to as AM/AM conversion.

A general AM/AM conversion characteristic curve is shown in figure 2.5. For relatively low level input voltages, the TWTA acts as a linear device. However, as the input voltage increases, the output voltage increases nonlinearly until the input drives the TWTA into full saturation. The input power at which output saturation occurs is

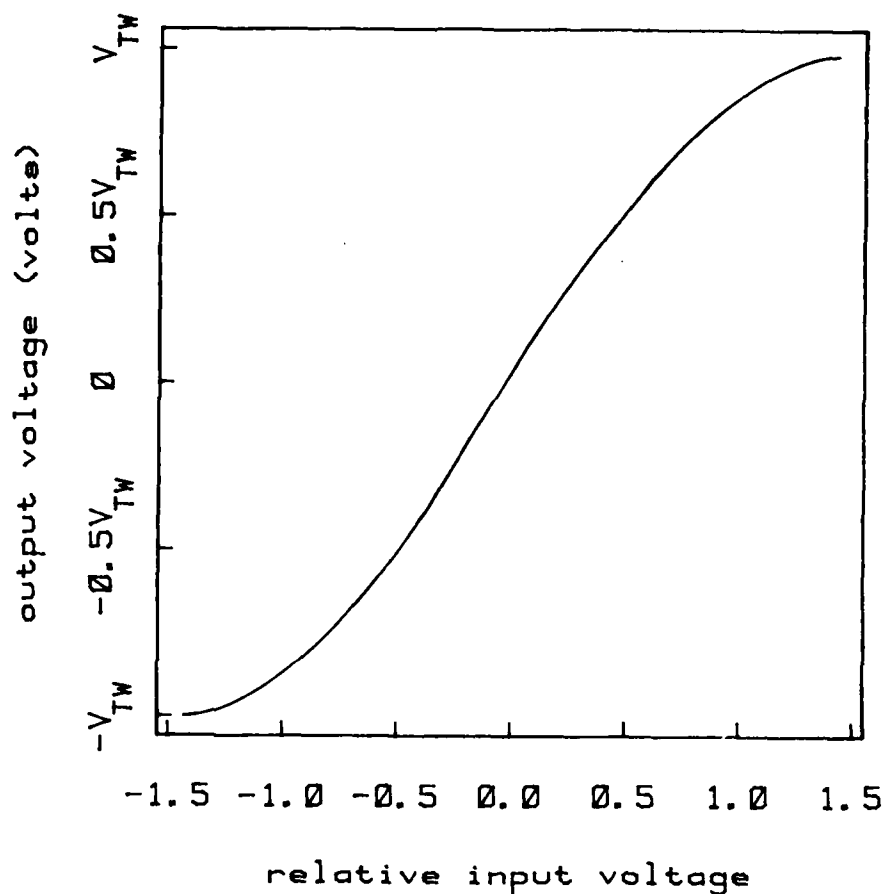


Fig. 2.5. TWTA AM/AM Conversion Characteristic Curve (1:174)

called the input saturation power. The ratio of the input saturation power to the desired input power is called the input backoff.

Increasing the input backoff decreases the output power but improves the linearity.

The maximum output power available from the TWTA is known as the output saturation power. The ratio of the output saturation power to actual output power is called the output backoff. An increase in the

input backoff causes an increase in the output backoff. The input backoff of the TWTA is controlled by the adjustable power amplifier preceeding the TWTA.

In some satellite links it may be desired that the TWTA operate at saturation. In a jamming environment, a linear operating TWTA can be caused to operate nonlinearly due to the additional input power from the jammer. The jammer thus causes AM/AM distortion to occur which causes a decrease in the downlink carrier-to-noise ratio. If the system were designed to operate at saturation, the jammer can no longer initiate the AM/AM distortion since it already exists.

For the case of a fully saturated transponder, the AM/AM conversion characteristic is modeled as a hard limiter. In the remaining analysis, this model of the TWTA shall be used.

In addition to the undesirable amplitude modulation caused by the TWTA, an undesirable phase modulation known as AM/PM conversion also exists. A typical AM/PM conversion characteristic curve is shown in figure 2.6. For an input to the TWTA of the form

$$x(t) = (A + \Delta(t))\cos(\omega t + \theta(t)) \quad (2.44)$$

The output phase, $\phi(t)$, is of the form

$$\phi(t) = \omega t + \theta(t) + \phi(\Delta(t)) \quad (2.45)$$

However, for a constant amplitude input (hard limiting prior to the TWTA; $\Delta(t)$ is a constant) the additional phase $\phi(\Delta(t))$ is a constant and is dealt with at the receiver.

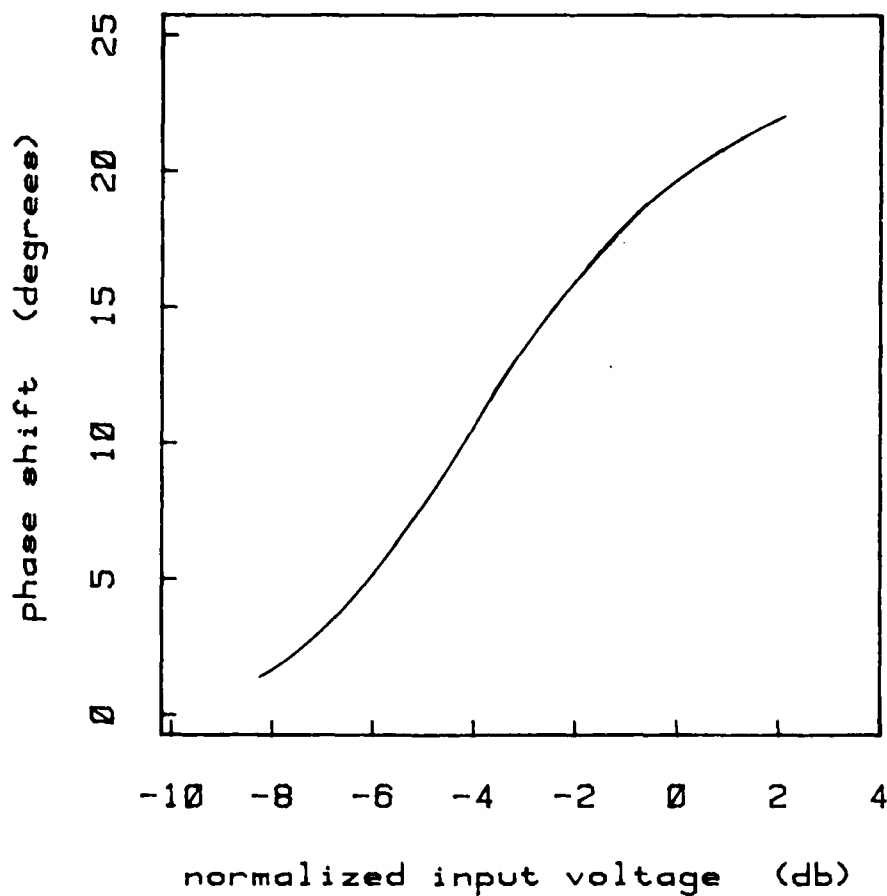


Fig. 2.6. TWTA AM/PM Conversion Characteristic Curve (1:178)

In summary, a satellite with a fully saturated TWTA can be modeled as having two band pass limiters in series. The first being an actual band pass limiter and the second being the TWTA operating at saturation.

The resulting downlink carrier-to-noise ratio for a single carrier input into a satellite with a fully saturated TWTA can be written as

$$(\text{CNR}_d)^{-1} = (\Gamma' \text{CNR}_u)^{-1} + (\text{CNR}_r)^{-1} \quad (2.46)$$

where

$$\Gamma' = \frac{\text{carrier-to-noise ratio out of TWTA}}{\text{uplink carrier-to-noise ratio}} = \frac{\text{CNR}_{\text{TWTA}}}{\text{CNR}_u} \quad (2.47)$$

which can be rewritten as

$$\Gamma' = \frac{(\pi/4)\Gamma e^{-\Gamma \text{CNR}_u} [I_0(\Gamma \text{CNR}_u/2) + I_1(\Gamma \text{CNR}_u/2)]^2}{1 - (\pi/4)\Gamma \text{CNR}_u e^{-\Gamma \text{CNR}_u} [I_0(\Gamma \text{CNR}_u/2) + I_1(\Gamma \text{CNR}_u/2)]^2} \quad (2.48)$$

where Γ is defined in Eq (2.40). This result is due to the fact that the input into the second BPL (TWTA) is ΓCNR_u and that

$$\Gamma' = \Gamma_{\text{BPL TWTA}} = (\text{CNR}_{\text{BPL}}/\text{CNR}_u)(\text{CNR}_{\text{TWTA}}/\text{CNR}_{\text{BPL}}) = \text{CNR}_{\text{TWTA}}/\text{CNR}_u \quad (2.49)$$

The adjustable power amplifier gain, g_2 , shown in figure 2.2, has no effect on the downlink carrier-to-noise ratio. This is because the carrier-to-noise ratio out of the amplifier and into the TWTA is identical to the carrier-to-noise ratio entering the amplifier. Since both the noise and the signal are amplified by an equal amount, the ratio of the two remains constant.

In Eq (2.46), the receiver carrier-to-noise ratio, CNR_r , is again defined as the ratio of the received signal power at the receiver to the received noise power at the receiver and is written as

$$\text{CNR}_r = P_{\text{so}} L_d / P_{\text{nd}} \quad (2.50)$$

where

$$P_{so} = (2V_T^2/\pi)\Gamma\text{CNR}_u e^{-\Gamma\text{CNR}_u} [I_0(\Gamma\text{CNR}_u/2) + I_1(\Gamma\text{CNR}_u/2)]^2 \quad (2.51)$$

The effects of having two BPL in series is shown in figure 2.7 with a graph of Γ' versus the uplink carrier-to-noise ratio, CNR_u . From this graph and the graph of figure 2.4, it is seen that

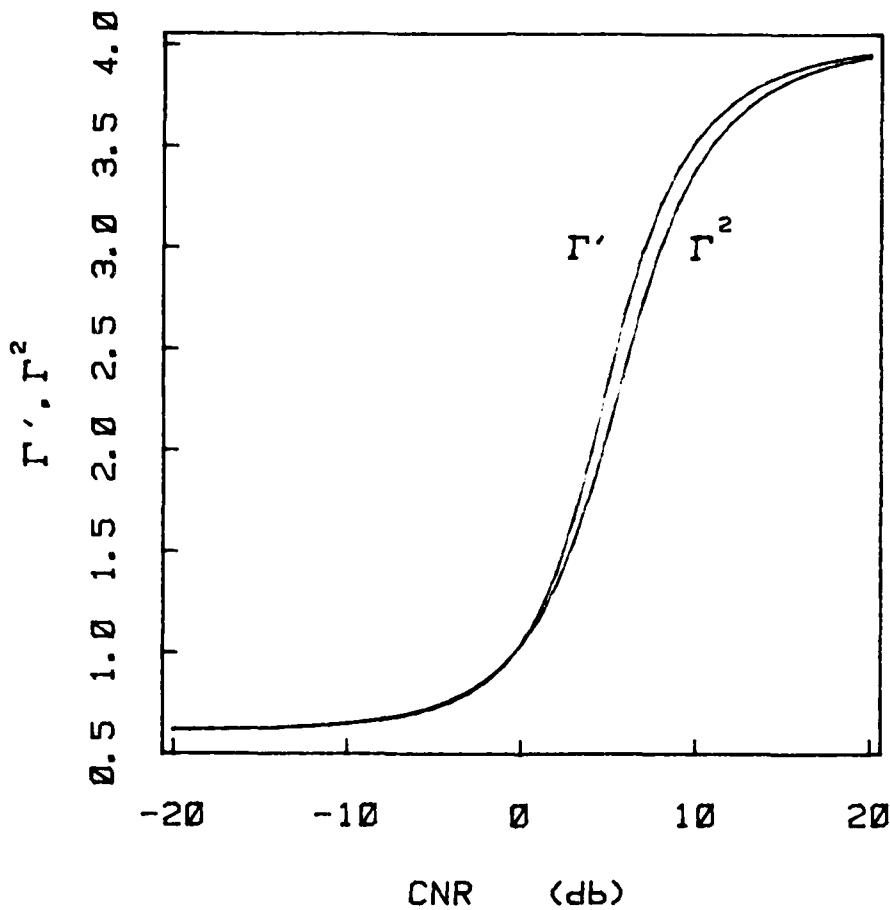


Fig. 2.7. Γ', Γ^2 Versus Uplink Carrier-to-Noise Ratio

two band pass limiters produce twice the effect of one band pass limiter. The graph of Γ' is basically the graph of $(\Gamma)^2$, as figure

2.7 shows. This can be explained by the fact that the BPL effects the uplink carrier-to-noise ratio by a maximum of 3db causing Γ_{TWTA} to differ only slightly from Γ_{BPL} , therefore $\Gamma' = \Gamma_{\text{BPL}} \Gamma_{\text{TWTA}} \approx \Gamma_{\text{BPL}}^2$.

In the next chapter, chapter 3, the fully saturated satellite transponder shall be analyzed with an input consisting of more than one carrier. However, first the remainder of this chapter shall discuss the concept of code-division multiple access communications.

Introduction to CDMA

In code division multiple access (CDMA) satellite communications systems, each uplink utilizes the entire satellite bandwidth and transmits to the satellite whenever desired. The links are separated by uniquely separable pseudo-random codes and require no time or frequency separation. If the code is modulated directly on the carrier, the format is referred to as direct sequence CDMA (DS-CDMA). If the code is used to continually change the carrier frequency, it is referred to as frequency hopped CDMA (FH-CDMA). The upcoming analysis deals only with DS-CDMA systems.

A simplified diagram of the DS-CDMA transmitter is shown in figure 2.8. The digital data to be transmitted is denoted by $d_i(t)$ ($d_i(t) = \pm 1$) where i signifies the i th uplink. The psuedo-random code is denoted by $q_i(t)$ ($q_i(t) = \pm 1$) with a chip time of T_q , where as $d_i(t)$ has a bit time of T_d , ($T_d \gg T_q$). The sequence, $q_i(t)$, is periodic with k binary symbols (chips) per period. It is

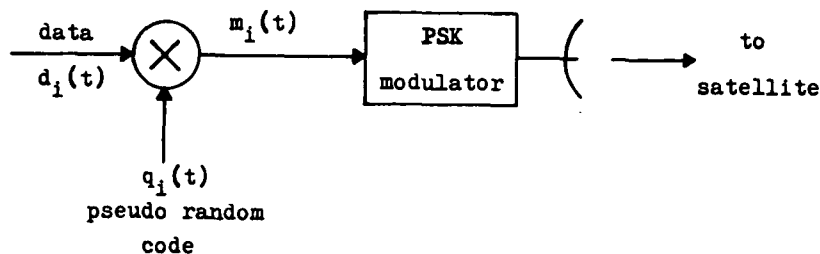


Fig. 2.8. Direct Sequence CDMA Modulator/Transmitter

generally the case that $T_d \leq kT_q$. That is, the data bit time is less than or equal to the pseudo-random code period.

The product of the data and the code, $m_i(t)$, is modulated by a BPSK modulator and transmitted to the satellite. Each earth station forms its PSK carrier in the same manner, each with the same rf frequency but with different pseudo-random codes. The satellite receives the sum of the transmitted signals and retransmits the sum back to the earth via a translated frequency band. The receiver then extracts the data which was intended for that specific user. Throughout this thesis, phase, frequency and time synchronizations are assumed even though synchronization is generally the limiting factor in CDMA performance.

A general diagram of a DS-CDMA receiver is shown in figure 2.9. The received signal, assuming an ideal linear satellite transponder

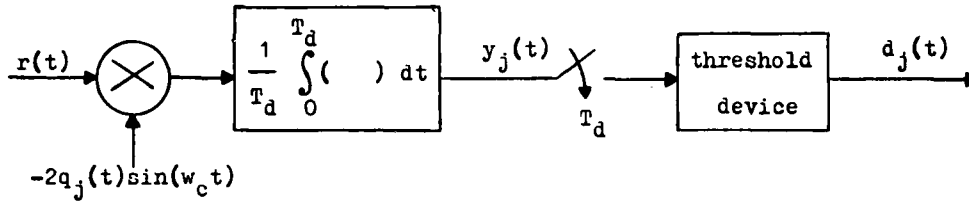


Fig. 2.9. Direct Sequence CDMA Demodulator/Receiver

with zero noise, is given by

$$r(t) = \sum_{i=1}^M A_i \sqrt{L_i} \cos(\omega_c t + \pi m_i(t)/2) \quad (2.52)$$

where

- A_i = transmitted carrier amplitude of i th link
- L_i = total uplink, downlink losses of i th link
- M = number of links accessing the satellite

Since $m_i(t) = \pm 1$, the received signal can be rewritten as

$$r(t) = - \sum_{i=1}^M A_i \sqrt{L_i} m_i(t) \sin(\omega_c t) \quad (2.53)$$

and the output of the integrator for the j th link, $y_j(t)$, can be written as

$$y_j(t) = T_d^{-1} \sum_{i=1}^M A_i \sqrt{L_i} \int_0^{T_d} m_i(t) q_j(t) dt \quad (2.54)$$

Since $d_i(t)$ is constant over the bit time, T_d , Eq (2.54) can be written as

$$y_j(t) = T_d^{-1} \sum_{i=1}^M A_i \sqrt{L_i} d_i \int_0^{T_d} q_i(t) q_j(t) dt \quad (2.55)$$

If the codes for each link are truly orthogonal, i.e.

$$T_d^{-1} \int_0^{T_d} q_i(t) q_j(t) dt = \begin{cases} 1, & i=j \\ 0, & i \neq j \end{cases} \quad (2.56)$$

then $y_j(t)$ can be further simplified to

$$y_j(t) = A_i \sqrt{L_j} d_j$$

where $d_j(t)$ can be derived from the sign of $y_j(t)$.

It is noted that many simplifying assumptions are made in the process of analyzing the DS-SSMA communication system. These assumptions are made to simplify the mathematics in showing the basic structure behind DS-SSMA communications. In the analysis to follow, the assumptions of receiver synchronization and orthogonal pseudo-random codes will still hold, whereas the assumptions of negligible noise and a linear satellite transponder will be dropped.

III. Hard Limiting of Multiple Carriers

In the latter section of chapter two, the concept of code-division multiple access satellite communication was introduced where multiple carriers are passed through the satellite transponder. This chapter is devoted to the carrier-to-noise ratio analysis of those CDMA signals. The analysis begins with the assumption of a linear satellite transponder and then moves onto the hard limiter transponder.

CDMA Link Analysis With Linear Transponder

In CDMA communications, each uplink can occupy the entire satellite bandwidth and the number of links, M , is limited by the effects of power sharing and the ability of obtaining M nearly orthogonal pseudo-random codes.

As shown in figure 3.1, the i th uplink power received at the front end of the satellite, P_{rui} , can be written as

$$P_{rui} = P_{sui} L_{ui} \quad (3.1)$$

where

P_{sui} = uplink transmit power of i th link

L_{ui} = uplink gains and losses of i th link = $g_{it} L_{aui} L_{pui} g_{ls}$

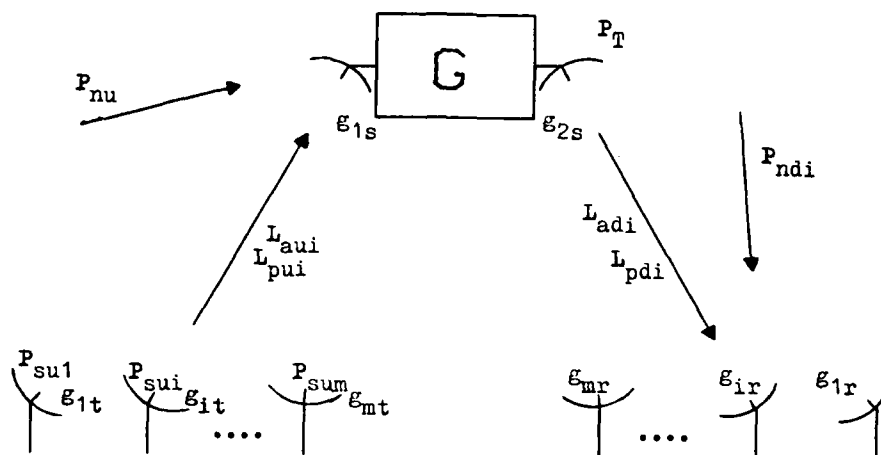


Fig. 3.1. Multilink Satellite Channel Model

The total noise power entering the satellite with an rf bandwidth of B_r is shown by Eq (2.8) to be

$$P_{nu} = kT_{eq} B_r = N_o B_r \quad (3.2)$$

Therefore, the total received uplink power entering the satellite,

P_{ru} , can be written as

$$P_{ru} = P_{nu} + \sum_{i=1}^M P_{sui} L_{ui} \quad (3.3)$$

For a linear transponder, the incoming signals are frequency translated and amplified by a gain of

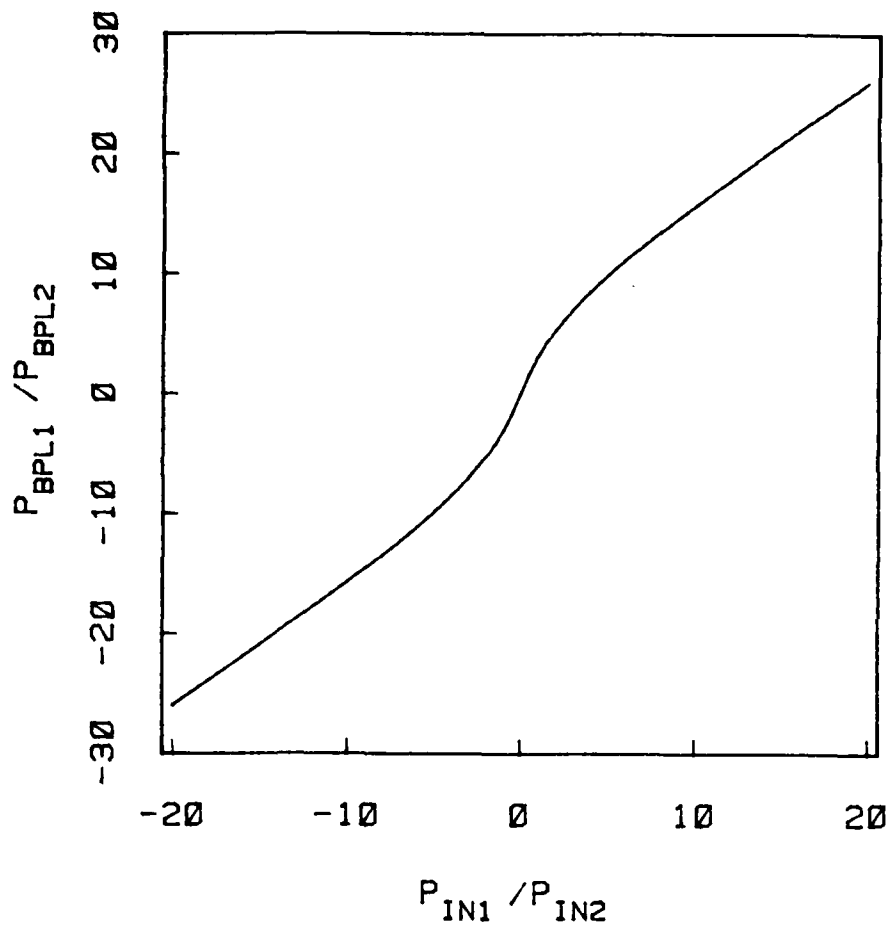


Fig. 4.1. BPL Output Power Ratio vs. Input Power Ratio (2 Links)

suppression can change the input power ratio, (P_{in1}/P_{in2}) , by as much as ± 6.0 db.

When two band-pass limiters are cascaded the effect is doubled as shown in figure 4.2. The carrier suppression can now reach ± 12 db.

IV. Verification of Preliminary Results

In chapter three, an equation was derived to determine the downlink carrier-to-noise ratio for M communication links accessing a satellite with a fully saturated TWTA. Since this equation is to be used to iteratively obtain the required uplink power needed to provide a specific downlink carrier-to-noise ratio, it is first important that the algorithm to obtain the downlink carrier-to-noise ratio be tested and verified with known results. This verification is accomplished by duplicating known results for the output of a single band-pass limiter. With the verification of these results, it can be assumed that the equations which produce the downlink carrier-to-noise ratio are valid, since the equations are the result of the cascade of two band-pass limiters.

Two Link Verification

For the case of two links accessing a satellite, with a high uplink carrier-to-noise ratio, the ratio of the band-pass limiter outputs for each link, (P_{BPL1}/P_{BPL2}) , versus the input power ratios, (P_{in1}/P_{in2}) , is shown in figure 4.1. This figure is identical to that obtained by Gagliardi (1,202). It is seen from figure 4.1 that the band-pass limiter attenuates weak signals and amplifies strong signals. This effect is referred to as carrier suppression and shows the disadvantage of simultaneously passing strong and weak signals through a band-pass limiter. This effect of carrier

$$\begin{aligned}
\text{CNR}_{di} &= P_{soi} 'L_{di} / (P_{no} 'L_{di} + P_{ndi}) = \\
&\frac{(8V_{TW}^2/\pi^2) \left[\int_0^\infty \omega^{-1} e^{-R_{no}(0)\omega^2/4P_{soi}} J_1(\omega) \prod_{j=1}^M J_0(\omega\sqrt{P_{soj}/P_{soi}}) d\omega \right]^2}{8V_{TW}^2/\pi^2 - \sum_{i=1}^M P_{soi} + P_{ndi}/L_{di}} \quad (3.41)
\end{aligned}$$

where

$$\begin{aligned}
L_{di} &= \text{ith link downlink losses} = (g_{2s} L_{adi} L_{pdi} g_{ir}) \\
P_{ndi} &= \text{ith link downlink noise} \\
R_{no}(0) &= \text{noise power out of BPL} = (8V_1^2/\pi^2 - \sum_{i=1}^M P_{soi}) \\
V_{TW} &= \text{TWTA voltage limit} \\
V_1 &= \text{BPL voltage limit} \\
P_{soi} &= \text{ith carrier signal power out of BPL, Eq (3.36)}
\end{aligned}$$

A signal-to-noise ratio per bit can easily be obtained from the downlink carrier-to-noise ratio and is given by

$$(E_b/N_o)_d = \text{CNR}_d T_b B_r = \text{CNR}_d B_r / R_d \quad (3.42)$$

where

$$\begin{aligned}
T_b &= \text{bit time duration} \\
B_r &= \text{satellite bandwidth} \\
R_d &= 1/T_b = \text{data rate}
\end{aligned}$$

Any subsequent analysis of the CDMA satellite system will use Eqs (3.41), (3.39), (3.37), and (3.36) to obtain the downlink carrier-to-noise ratio given various transmit powers and other needed parameters.

where

$$\begin{aligned} V_{TW} &= \text{TWTA voltage limit} \\ R_{no}(0) &= \text{output noise power from BPL} \\ P_{soi} &= \text{output signal power from BPL for } i\text{th link} \end{aligned}$$

With a change of variable, $\beta = \omega^2 g_2$, the signal power can be simplified to yield

$$\begin{aligned} P_{soi}' &= (8V_{TW}^2/\pi^2) \left[\int_0^\infty \beta^{-1} e^{-R_{no}(0)\beta^2/4P_{soi}} J_1(\beta) \right. \\ &\quad \times \left. \prod_{\substack{j=1 \\ j \neq i}}^M J_0(\beta \sqrt{P_{soj}/P_{soi}}) d\omega \right]^2 \quad (3.39) \end{aligned}$$

Neither the ratio $(R_{no}(0)/P_{soi})$ nor (P_{soj}/P_{soi}) contains the magnitude of the band-pass limiter, V_1 . Also, the adjustable amplifier gain is no longer present in the signal power equation. Thus, the level of the band-pass limiter and the amplifier gain, g_2 , have no effect on the TWTA output power.

The output noise power of the TWTA can now be written as

$$P_{no}' = (8V_{TW}^2/\pi^2 - \sum_{i=1}^\infty P_{soi}') \quad (3.40)$$

The downlink carrier-to-noise ratio for the i th link can finally be written as

$$P_{soi} = (8V_1^2/\pi^2) \left[\int_0^\infty \omega^{-1} e^{-R_n(0)\omega^2/2} J_1(\omega A_1 \sqrt{L_{u1}}) \right. \\ \left. \times \prod_{\substack{j=1 \\ j \neq i}}^M J_0(\omega A_j \sqrt{L_{uj}}) d\omega \right]^2 \quad (3.36)$$

The noise is zero mean and gaussian with variance $R_{no}(0)$, where

$$R_{no}(0) = P_{no} = (8V_1^2/\pi^2 - \sum_{i=1}^M P_{soi}) \quad (3.37)$$

With the analysis for the band-pass limiter complete, it is relatively simple to obtain the output signal and noise power for the TWTA since it is also assumed to be operating at saturation.

The input to the TWTA is a sum of sinusoids, Eq (3.35), plus zero mean, gaussian, narrow band noise with a noise power of $g_2 R_{no}(0)$ where g_2 is the gain of the adjustable power amplifier as shown in figure 2.2.

From previous results, Eqs (3.23) and (3.33), the output signal power for the i th link can now be written as

$$P_{soi}' = (8V_{TW}^2/\pi^2) \left[\int_0^\infty \omega^{-1} e^{-R_{no}(0)\omega^2/2} J_1(\omega \sqrt{2P_{soi} g_2}) \right. \\ \left. \times \prod_{\substack{j=1 \\ j \neq i}}^M J_0(\omega \sqrt{2P_{soj} g_2}) d\omega \right]^2 \quad (3.38)$$

total output power and the desired signal power is known. From Eq (3.23), the total output signal power, P_{so} , from the band-pass limiter is written as

$$P_{so} = \sum_{i=1}^M P_{soi} \quad (3.32)$$

The total output noise power consisting of thermal noise and intermodulation noise can now be written as

$$P_{no} = P_t - P_{so} = (8V_1^2/\pi^2 - \sum_{i=1}^M P_{soi}) \quad (3.33)$$

In summary, for a CDMA input of the form

$$r(t) = \sum_{i=1}^M A_i \sqrt{L_i} \cos(\omega_c t + \pi m_i(t)/2) \quad (3.34)$$

with zero mean, gaussian, narrow band noise, the output of the band-pass limiter, consists of a desired signal plus noise. The desired output signal term can be written as

$$y(t) = \sum_{i=1}^M \sqrt{2P_{soi}} \cos(\omega_c t + \pi m_i(t)/2) \quad (3.35)$$

where

$$N_3 = N_{1,1,1}^3 + N_{1,2}^3 = M(M-1)M/2 \quad (3.31)$$

As the order of intermodulation increases the actual amplitude of the intermodulation decreases due to the product of additional cosine terms, each of which decreases the magnitude by a factor of two. In general, Shaft has shown that the power in the intermodulation terms of the third, fifth, ..., nth order decreases by a factor of M^3, M^5, \dots, M^n where M is the total number of carriers (5:508).

At this point, a simplifying assumption is made about the intermodulation produced by the band-pass limiter. It is assumed that the intermodulation can be treated as additional gaussian noise with zero mean. This assumption follows from the central limit theorem, (4:266), and the fact that the total intermodulation power is due to an infinite summation of individual intermodulation terms as shown in Eq (3.19).

Since the intermodulation is made up of sums of products of sinusoids whose phases consist of pseudo-random sequences, it is logical to assume that the intermodulation has zero mean. However, for the central limit theorem to be valid, the intermodulation noise must be comprised of many independent components. The intermodulation is comprised of many components but they are most likely not independent. Regardless of the independence, the assumption is used to simplify the mathematics in determining the output of the TWTA.

With the previous assumptions, the output of the band-pass limiter can be assumed to be the desired output plus gaussian noise. The variance or power of the gaussian noise can now be found since the

when one n_i equals two, another n_i equals one and the remaining n_i 's are zero. The product of three carriers produces a sum of four cosines whose arguments are the sum and differences of each individual argument as shown below.

$$\begin{aligned} \cos(\omega_c t + \theta_i) \cos(\omega_c t + \theta_j) \cos(\omega_c t + \theta_k) = (1/4) [\cos(3(\omega_c t + \theta_i + \theta_j + \theta_k)) \\ + \cos(\omega_c t + \theta_i + \theta_j - \theta_k) + \cos(\omega_c t + \theta_i - \theta_j + \theta_k) + \cos(\omega_c t - \theta_i + \theta_j + \theta_k)] \end{aligned} \quad (3.27)$$

The last three cosines are passed by the band-pass filter. The total number of third order intermodulations created by the product of three sinusoids of the combination given in Eq (3.27) is given by

$$N_{3,1,1} = 3(M!)/3!(M-3)! = M(M-1)(M-2)/2 \quad (3.28)$$

The second intermodulation of the third order is produced by the combination of $m_i=2$ and $m_j=1$ and is given by

$$\begin{aligned} \cos(2(\omega_c t + \theta_i)) \cos(\omega_c t + \theta_j) = \frac{1}{2} [\cos(3\omega_c t + 2\theta_i + \theta_j) \\ + \cos(\omega_c t + 2\theta_i - \theta_j)] \end{aligned} \quad (3.29)$$

The last cosine is the only one passed by the band-pass filter. The total number of intermodulations due to the above combination is given as

$$N_{3,1,2} = (M!)/(M-2)! = M(M-1) \quad (3.30)$$

The total number of third order intermodulations, N_3 , is the sum of Eqs (3.28) and (3.30) which yields

$$P_{\text{sol}} = (8V_1^2/\pi^2) \left(\int_0^\infty \omega^{-1} e^{-R(0)\omega^2/2} \prod_{j=1}^M J_1(\omega a_j) J_0(\omega a_j) d\omega \right)^2 \quad (3.23)$$

Since the input of many sinusoids and narrowband noise can be written as one sinusoid with a very complex amplitude and phase, the total output power of the BPL is seen from Eq (2.26) to be

$$P_t = 8V_1^2/\pi^2 \quad (3.24)$$

This total power is comprised of the desired output signal power plus two undesirable forms of power. The first undesirable power is the power due to the input thermal noise and the second is the power due to the intermodulation products that get passed by the band-pass limiter. From Eq (3.19), an intermodulation product is passed by the BPF if

$$n_1 \pm n_2 \pm \dots \pm n_M = \pm 1 \quad (3.25)$$

which only occurs when

$$\sum_{i=1}^M n_i = \pm a \quad (3.26)$$

where

$$a = \text{order of modulation} = 1, 3, 5, 7, \dots$$

The number of intermodulation products becomes very large as the order of intermodulation increases. Third order intermodulation occurs when three of the n_i 's equal one with the others being zero or

The codes produced in the additional terms are not orthogonal to the designed codes. Therefore, upon decoding, interference is produced due to the hard limiter.

The output signal power can now be written for the i th signal by letting $\tau=0$, $m_i=1$, $m_{j \neq i}=0$, and $k=0$ in Eqs (3.13) and (3.16), and is given by

$$P_{\text{sol}} = 2h_0^2(0, \dots, 0, 1, 0, \dots, 0) \quad (3.20)$$

where

$$h_0(0, \dots, 0, 1, 0, \dots, 0) = (V_1/\pi) \int_{-\infty}^{\infty} \omega^{-1} e^{-R_n(0)\omega^2/2} J_1(\omega a_1) \times \prod_{\substack{j=1 \\ j \neq 1}}^M J_0(\omega a_j) d\omega \quad (3.21)$$

Since $J_1(\omega)$ and ω^{-1} are odd functions and $J_0(\omega)$ and $\exp(-R_n(0)\omega^2/2)$ are even functions, the entire integrand is an even function and the integrand can be simplified to

$$h_0(0, \dots, 0, 1, 0, \dots, 0) = (2V_1/\pi) \int_0^{\infty} \omega^{-1} e^{-R_n(0)\omega^2/2} J_1(\omega a_1) \prod_{\substack{j=1 \\ j \neq 1}}^M J_0(\omega a_j) d\omega \quad (3.22)$$

The output signal power for the i th link can now be written as

$$h_k(m_1, m_2, \dots, m_M) = (V_1/\pi) \int_{-\infty}^{\infty} \omega^{k-1} e^{-R_n(0)\omega^2/2} \prod_{j=1}^M J_{m_j}(\omega a_j) d\omega$$

$$\times \prod_{i=1}^M J_{m_i}(\omega a_i) d\omega \quad (3.16)$$

From Eqs (3.15) and (A.3), the output of a hard limiter with an input of M binary phase shift keyed signals with identical frequencies can be written as

$$y(t) = (V_1/j\pi) \int_{-\infty}^{\infty} \omega^{-1} \exp(j\omega \sum_{i=1}^M a_i \cos(\omega_c t + \theta_i)) d\omega \quad (3.17)$$

Using the Jacobi-Anger identity, Eq (A.8), the output can be rewritten as

$$y(t) = (V_1/j\pi) \int_{-\infty}^{\infty} \omega^{-1} \prod_{i=1}^M \sum_{n=0}^{\infty} \epsilon_n I_n(j\omega a_i) \cos(n(\omega_c t + \theta_i)) d\omega \quad (3.18)$$

and can be further simplified to

$$y(t) = (V_1/j\pi) \sum_{n_1=0}^{\infty} \sum_{n_2=0}^{\infty} \dots \sum_{n_M=0}^{\infty} \prod_{i=1}^M [\epsilon_{n_i} \cos(n_i(\omega_c t + \theta_i))] \times \int_{-\infty}^{\infty} \omega^{-1} I_{n_1}(j\omega a_1) d\omega \quad (3.19)$$

The desired output signal for the i th carrier occurs when $n_i=1$ and $n_{j \neq i}=0$. The product of cosines will produce additional terms which are passed by the bandpass filter following the hard limiter.

$$R_y(\tau) = \sum_{k=0}^{\infty} (-1)^k R_n^k(\tau)/k! \sum_{m_1=0}^{\infty} \sum_{m_2=0}^{\infty} \dots \sum_{m_M=0}^{\infty} \epsilon_{m_1} \epsilon_{m_2} \dots \epsilon_{m_M} h_k^2(m_1, m_2, \dots, m_M) \times \prod_{i=1}^M \cos(\omega_c \tau - \theta_i(t) + \theta(t+\tau)) \quad (3.13)$$

where

$$h_k(m_1, m_2, \dots, m_M) = (2\pi)^{-1} \int_{-\infty}^{\infty} G(\omega) \omega^k e^{-R_n(0)\omega^2/2} \prod_{j=1}^M (\omega a_j)^{m_j} J_{m_j}(\omega a_j) d\omega \quad (3.14)$$

a_i = input carrier amplitude of i th link = $A_i \sqrt{L_{ui}}$

$$\epsilon_m = \begin{cases} 1, & m = 0 \\ 2, & m = 1, 2, 3, \dots \end{cases}$$

For the two hard limiters encountered in the satellite transponder, (BPL, TWT), the fourier transform of the hard limiter input/output characteristic, figure 2.3, is given as

$$G(\omega) = 2V_1/j\omega \quad (3.15)$$

where V_1 is the amplitude level of the limiter. Eq (3.14) can now be simplified to

The receiver carrier-to-noise ratio can also be written as

$$CNR_{ri} = (P_{T_{ui}} L_{di} / P_{ndi}) (P_{sui} / P_{ru}) \quad (3.11)$$

where P_{ru} is the total received uplink power. Eq (3.11) clearly shows the effects of power sharing in the satellite. As more links try to access the satellite, the ratio (P_{sui} / P_{ru}) decreases causing a decrease in both the receiver and downlink carrier-to-noise ratios. The same effect occurs if any link other than the i th link increases its transmitted power.

Analysis of Hard Limited CDMA Signals

As was shown in chapter 2, the total CDMA signal entering the satellite with BPSK signalling is written as

$$r(t) = \sum_{i=1}^M A_i \sqrt{L_{ui}} \cos(\omega_c t + \pi m_i(t)/2) \quad (3.12)$$

where

- A_i = uplink carrier amplitude of i th link
- L_{ui} = uplink gains and losses of i th link = $g_{it} L_{aui} L_{pui} g_{ls}$
- $m_i(t)$ = product of data sequences and pseudo-random code for i th link

For a hard limiter with an input consisting of BPSK multiple carrier signals of identical frequency and independent, zero mean, additive white gaussian noise, the output autocorrelation is shown in appendix A, Eqs (A.31) and (A.32), to be

$$G = P_T/P_{ru} = P_T/(P_{nu} + \sum_{i=1}^M P_{sui} L_{ui}) \quad (3.4)$$

where P_T is the total available transmit power of the satellite prior to the transmit antenna. The total received carrier power of the i th link, P_{rdi} , is then written as

$$P_{rdi} = P_{sui} L_{ui} L_{di} G = P_{sui} L_{ui} L_{di} P_T / (P_{nu} + \sum_{j=1}^M P_{suj} L_{uj}) \quad (3.5)$$

The total received noise power of the i th link is composed of a downlink noise power and an uplink noise power which is retransmitted with the desired signal to the downlink receiver. The sum of these two noise powers can be written as

$$P_{nti} = P_{nu} L_{di} + P_{ndi} = [P_{nu} L_{di} P_T / (P_{nu} + \sum_{j=1}^M P_{suj} L_{uj})] + P_{ndi} \quad (3.6)$$

The downlink carrier-to-noise ratio for the i th link, CNR_{di} , can now be formed and is given by

$$CNR_{di} = P_{rdi}/P_{nti} = P_{sui} L_{ui} L_{di} G / (P_{nu} L_{di} + P_{ndi}) \quad (3.7)$$

which can be rewritten as

$$(CNR_{di})^{-1} = (CNR_{ui})^{-1} + (CNR_{ri})^{-1} \quad (3.8)$$

where

$$CNR_{ui} = \text{uplink CNR of } i\text{th link} = P_{sui} L_{ui} / P_{nu} \quad (3.9)$$

$$CNR_{ri} = \text{receiver CNR of } i\text{th link} = P_{sui} L_{ui} L_{di} G / P_{ndi} \quad (3.10)$$

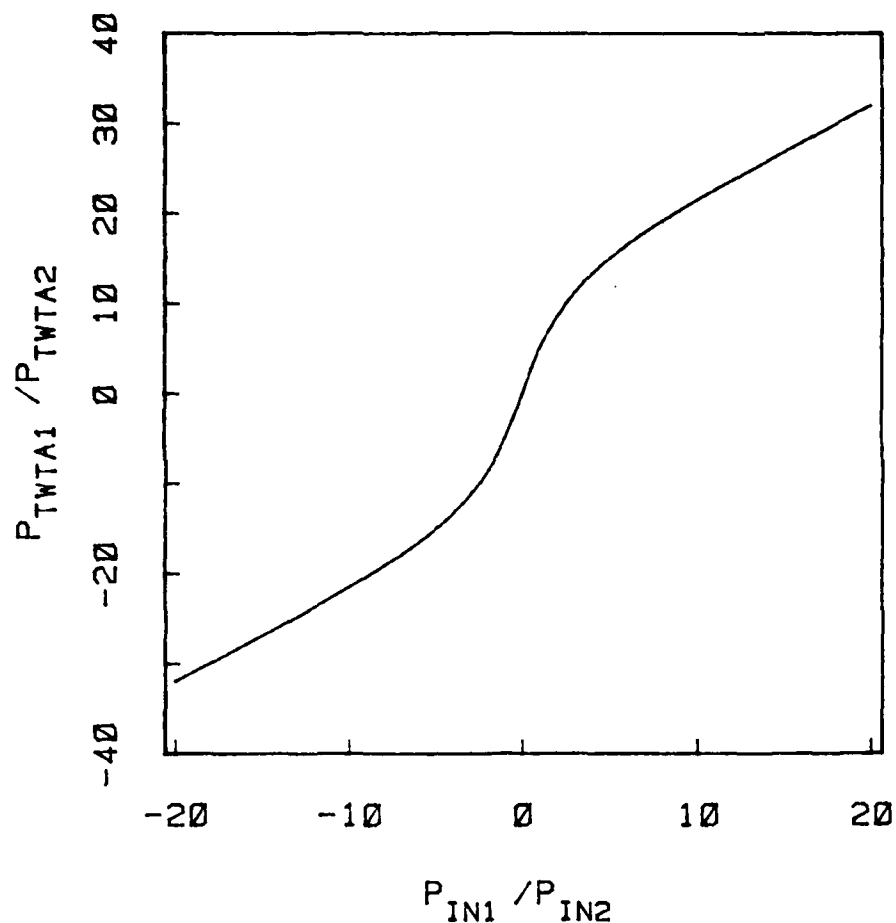


Fig. 4.2. TWTA Output Power Ratio vs. BPL Input Power Ratio (2 Links)

Four Link Verification

Additional algorithm verification was accomplished with four link accessing the satellite. The output power and signal suppression is plotted versus the input power ratio of (P_{in2}/P_{in4}) . The input consists of two large signals of equal amplitude and two small signals of equal amplitude. Each graph contains two plots with an uplink carrier-to-noise ratio of ± 10.0 db.

The graph of the band-pass output power is shown in figure 4.3 and the graph of the signal suppression is shown in figure 4.4. The graphs closely resemble those obtained by Shaft (5:507). An interpretation of the graphs is given by Shaft and is not repeated here.

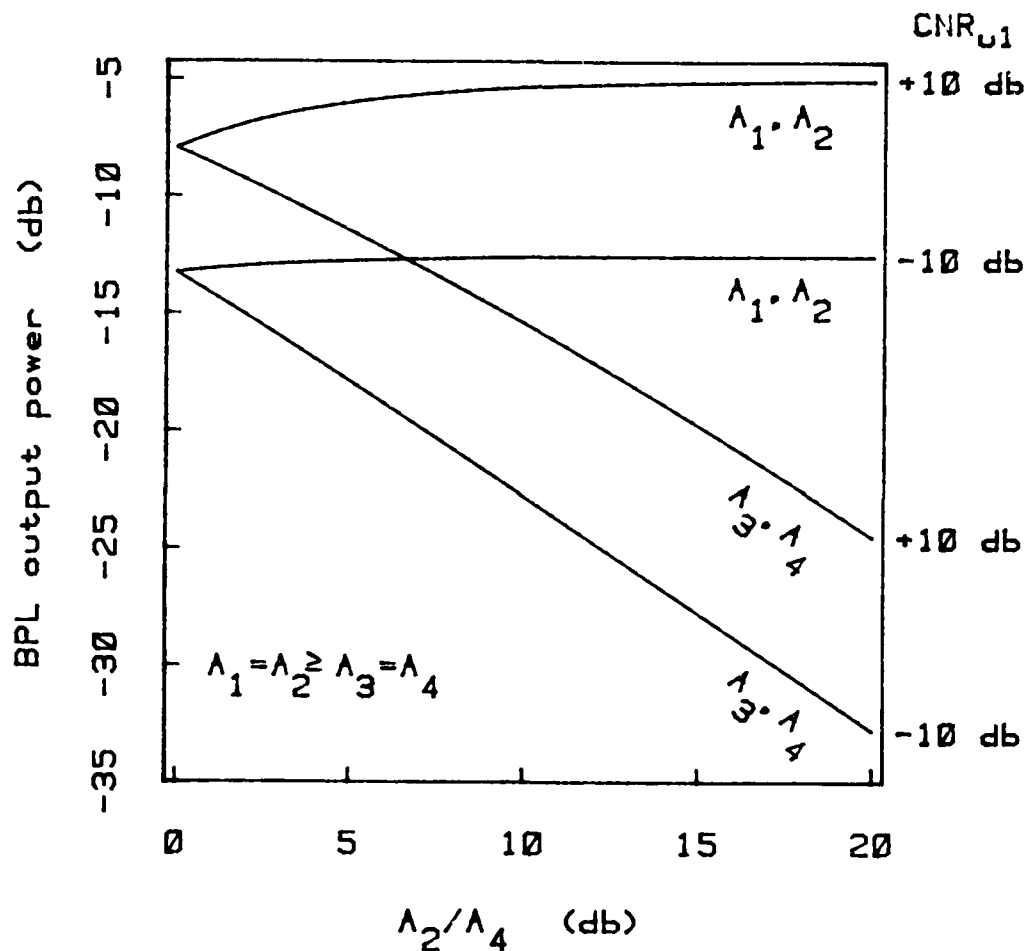


Fig. 4.3. BPL Output Power vs. Input Power Ratio (4 Links)

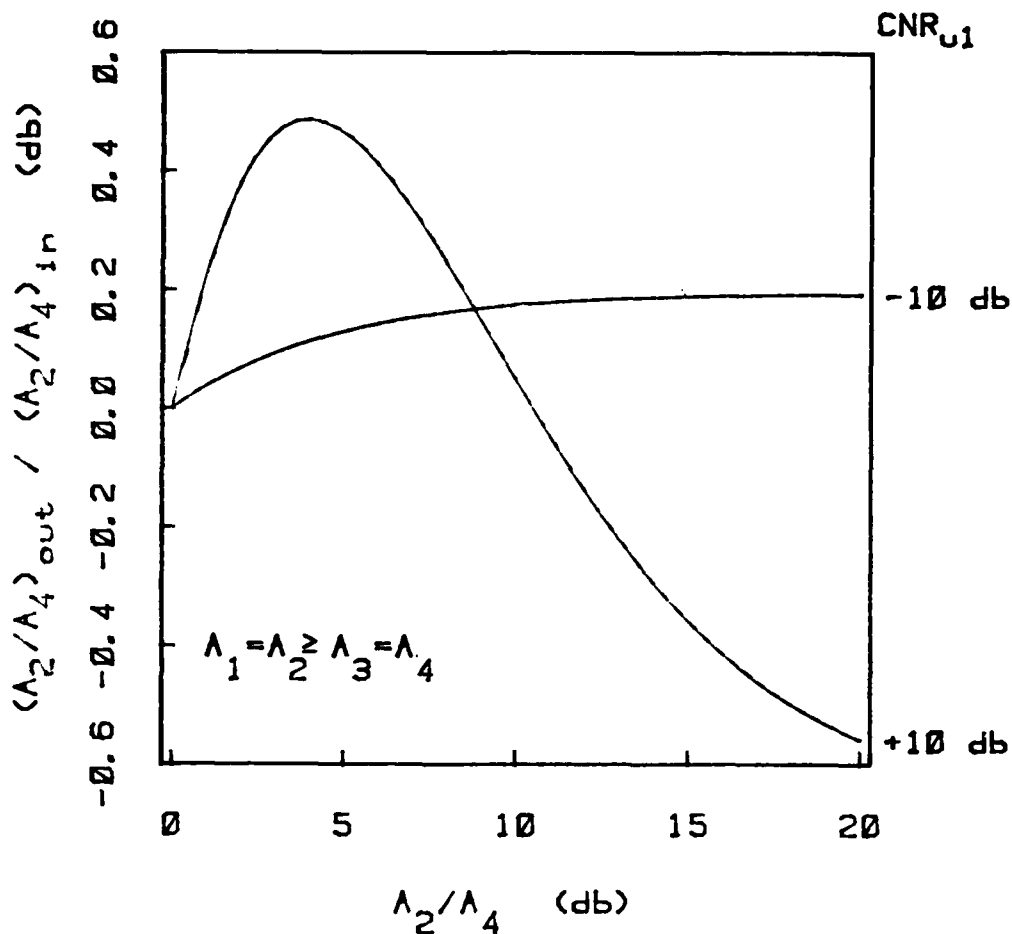


Fig. 4.4. BPL Signal Suppression vs. Input Power Ratio (4 Links)

From the graphs of figures 4.1 through 4.4 and the graphs of Gaglaridi and Shaft, it is assumed that the algorithm which calculates the output of a band-pass limiter is valid. With this algorithm, the downlink carrier-to-noise ratio can be found since the satellite is modeled as the cascade of two band-pass limiters.

V. Margin Leveling Algorithm

The main goal of this thesis is to find the proper uplink transmit powers which yield the required downlink margins given various size earth terminal antennas and a fully saturated satellite transponder. The equations derived in chapter three perform the inverse of the desired operation. Given the various parameters including the uplink transmit power, the equations can be used to calculate the associated downlink carrier-to-noise ratios. Since the downlink carrier-to-noise ratio equation, Eq (3.39), is analytically non-invertable due to the integrand of the product of M Bessel functions, a method of numerical inversion is required.

Prior to the discussion of the margin leveling algorithm, it is first essential to understand the three scenarios for which the algorithm is designed for.

Margin Leveling Scenarios

The first and simplest scenario is when margin leveling is needed since the uplink transmit powers required to achieve the desired margins are less than or equal to the maximum uplink transmit powers. For this case, the desired margin and the obtained margin are equivalent.

The second and third scenarios are those requiring margin leveling with the difference in the two being the type of leveling desired. The second scenario, which is by far the simpler of the two, requires only the leveling of the unachievable margins. The third

scenario requires the leveling of all margins by an equal amount until each margin is achieved. In either case, the difference between the desired and the obtained margin must be kept to a minimum.

The second scenario is desired if it is not essential that each link remains fully operational. If the leveled margin for a particular link becomes too low to achieve reliable communication in a jamming environment, this link can be taken off line to provide more TWTA power to the other users.

The third scenario is desired if it is essential that each link remains in operation. Since margin leveling is performed on all links whether they achieve the desired margin or not, the leveled margins for those links initially not achieving the desired margin will be greater than the leveled margins of the second scenario. The lower leveled margins for the third scenario are due to the power sharing effects occurring in the TWTA. When a link which initially achieved the desired margin is leveled, it requires less TWTA power to achieve the new margin, thus allowing more TWTA power for those links not initially achieving their desired margins.

Margin Leveling Algorithm

The margin leveling algorithm to be discussed is shown in figure 5.1. After reading in the proper link parameters set by the user, the algorithm computes the margins obtained when the uplink transmit powers are maximized. With the initial slope set at 1.0, a new set of uplink powers are created via linear interpolation from the margins at maximum uplink power. If any uplink power exceeds its maximum, then

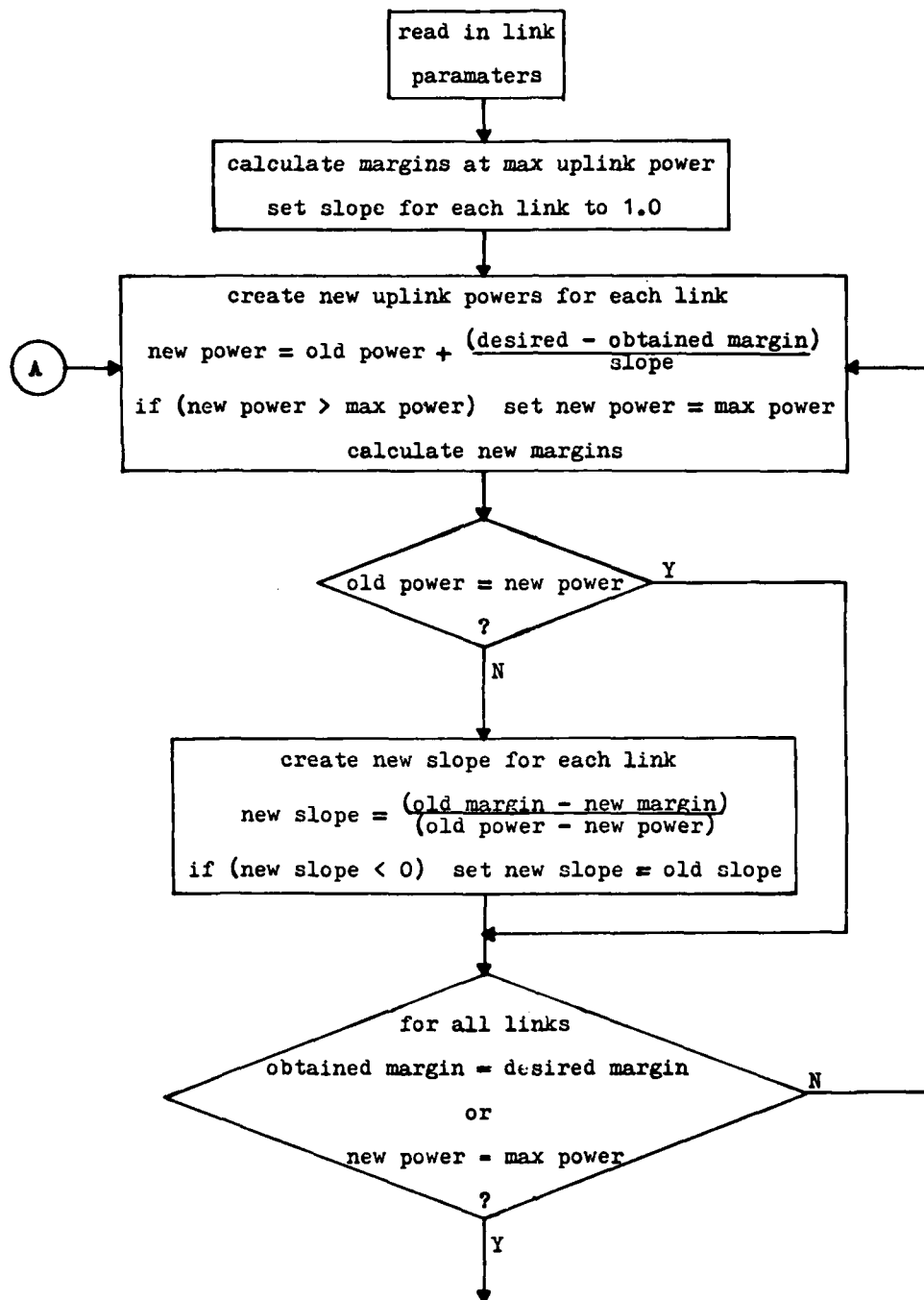


Fig. 5.1a Margin Leveling Algorithm (Convergence Routine)

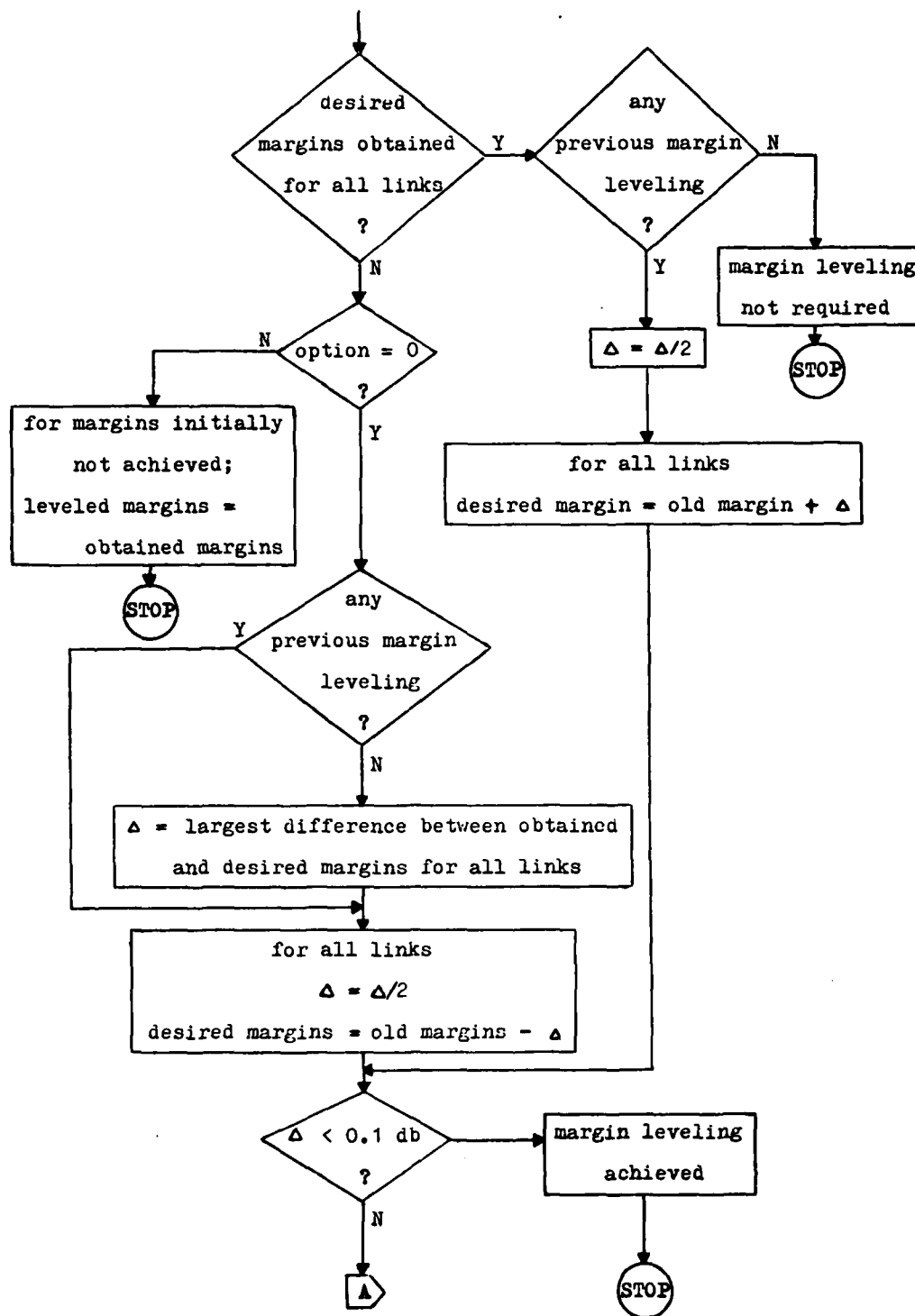


Fig. 5.1b Margin Leveling Algorithm (Leveling Routine)

that uplink power is set to the maximum level for that link. This situation occurs when a particular link margin is unachievable.

With the creation of new uplink powers, a new set of margins are determined. At this point, the slope is updated if the old and new powers are not equivalent. This prevents the occurrence of an infinite slope which would have occurred when an uplink power is maximized on consecutive passes through the convergence routine. When this situation arises, the prior slope is maintained.

Due to the power sharing which takes place in the satellite, it is possible that a negative slope may occur. For example, a situation may occur where the uplink power of a high power link is increased by a large amount and that of a smaller power link is increased only slightly. When this occurs, the larger link will "rob" some power from the smaller link. Even though the uplink power for the smaller link was increased, the new margin may be less than the old, causing a negative slope for that smaller link. At this point the obtained margin is still less than the desired margin for the small link and more power is needed to increase the obtained margin. However, if the negative slope is utilized in determining the new uplink power, the new power will be less than the old power which is highly undesirable. The negative slope tends to cause non-convergence of the leveling routine and for this reason when a negative slope occurs it is ignored and the prior slope is maintained.

Once the new slope is obtained or the old slope is retained, the convergence routine continues to create new uplink powers and downlink margins until the obtained margins are within 0.2 db of the desired

margins or the uplink powers are maximized. One of these criteria must be simultaneously satisfied for each link before program execution continues beyond the margin convergence routine.

If every margin converges to the desired margin, then the uplink powers which provide the desired margins are known and no margin leveling is required. However, if every desired margin is not achieved, then margin leveling is performed as specified by the option selected by the user. Since option zero is relatively simple its algorithm is discussed first.

With option zero selected, the algorithm performs margin leveling on those links which have not achieved the desired margins. With the completion of the margin convergence routine, the uplink powers for those links are maximized. This, in turn, has caused the associated margins to be maximized also. Therefore, the margins satisfy the criteria of having a minimum difference between the desired and the leveled margins. Margin leveling is therefore achieved by letting the leveled margins equal the obtained margins. The associated uplink powers for the leveled margins are those used to create their respective margins.

For the remaining option, option one, margin leveling is performed on each link by an equal amount until the difference between the desired and the leveled margin is minimal. The difference becomes minimal only when one uplink power becomes maximized.

After the margin convergence routine has been completed for the first time, the largest difference, delta, between the obtained margin and the desired margin is obtained. Each desired margin is then

decremented by half of this largest difference. There is no need to decrement by the largest difference since this set of margins would definitely be achieved but would not provide the minimum difference between the desired and leveled margins.

At this point, program execution returns to the margin convergence routine where either all the links obtain the new margins or at least one link does not. If every new margin is achieved, the margins are then incremented by half of the previous delta. If one or more links do not achieve the new margins, the margins are then decremented by half of the prior delta.

The above procedure continues until delta is small enough to be neglected. The end result is a set of leveled margins which differ by the desired margins by an equal amount for each link.

The execution of the margin leveling algorithm is illustrated via a computer printout in figure 5.2 for the simple case of two links. The link number, the uplink power (PWR), the obtained margin (OMARG), the desired margin (DMARG), and the slope (A) are listed to show the progression of the algorithm. The uplink power and the margins are shown in decibels. The skipped lines in figure 5.2 correspond to the point in the algorithm where margin convergence or maximum power has simultaneously occurred for each link.

The maximum power is shown in the first two lines to be 34.0 and 27.7 db for the first and second link respectively. At the end of the first convergence it is seen that the first link has achieved the desired margin but the second link has not. However, the uplink power of the second link is maximized. If option zero were chosen instead

1	FWR=	.3400E+02	OMARG=	.4496E+02	DMARG=	.2660E+02	A=	.1000E+01
2	FWR=	.2770E+02	OMARG=	.3180E+01	DMARG=	.2660E+02	A=	.1000E+01
1	FWR=	.3372E+02	OMARG=	.4498E+02	DMARG=	.2660E+02	A=	.1000E-01
2	FWR=	.2770E+02	OMARG=	.2899E+01	DMARG=	.2660E+02	A=	.1000E+01
1	FWR=	.2071E+02	OMARG=	.3870E+02	DMARG=	.2660E+02	A=	.5475E-01
2	FWR=	.2770E+02	OMARG=	.1045E+02	DMARG=	.2660E+02	A=	.1000E+01
1	FWR=	.7699E+01	OMARG=	.1983E+02	DMARG=	.2660E+02	A=	.3327E+00
2	FWR=	.2770E+02	OMARG=	.2849E+02	DMARG=	.2660E+02	A=	.1000E+01
1	FWR=	.1057E+02	OMARG=	.2385E+02	DMARG=	.2660E+02	A=	.1351E+00
2	FWR=	.2770E+02	OMARG=	.2513E+02	DMARG=	.2660E+02	A=	.1527E+01
1	FWR=	.1289E+02	OMARG=	.2816E+02	DMARG=	.2660E+02	A=	.2524E+00
2	FWR=	.2770E+02	OMARG=	.2119E+02	DMARG=	.2660E+02	A=	.1527E+01
1	FWR=	.1193E+02	OMARG=	.2628E+02	DMARG=	.2660E+02	A=	.3026E+00
2	FWR=	.2770E+02	OMARG=	.2293E+02	DMARG=	.2660E+02	A=	.3961E+00
1	FWR=	.1208E+02	OMARG=	.2656E+02	DMARG=	.2660E+02	A=	.2686E+00
2	FWR=	.2770E+02	OMARG=	.2266E+02	DMARG=	.2660E+02	A=	.3961E+00
1	FWR=	.1116E+02	OMARG=	.2486E+02	DMARG=	.2463E+02	A=	.2422E+00
2	FWR=	.2770E+02	OMARG=	.2422E+02	DMARG=	.2463E+02	A=	.3961E+00
1	FWR=	.1105E+02	OMARG=	.2467E+02	DMARG=	.2463E+02	A=	.2072E+00
2	FWR=	.2770E+02	OMARG=	.2440E+02	DMARG=	.2463E+02	A=	.3961E+00
1	FWR=	.1050E+02	OMARG=	.2374E+02	DMARG=	.2365E+02	A=	.1893E+00
2	FWR=	.2770E+02	OMARG=	.2522E+02	DMARG=	.2365E+02	A=	.3961E+00
1	FWR=	.1045E+02	OMARG=	.2366E+02	DMARG=	.2365E+02	A=	.1725E+00
2	FWR=	.2770E+02	OMARG=	.2530E+02	DMARG=	.2365E+02	A=	.3961E+00
1	FWR=	.1044E+02	OMARG=	.2665E+02	DMARG=	.2365E+02	A=	.1546E+00
2	FWR=	.2770E+02	OMARG=	.2531E+02	DMARG=	.2365E+02	A=	.3961E+00
1	FWR=	.1044E+02	OMARG=	.2365E+02	DMARG=	.2365E+02	A=	.1444E-01
2	FWR=	.2770E+02	OMARG=	.2531E+02	DMARG=	.2365E+02	A=	.5822E-04
1	FWR=	.1044E+02	OMARG=	.3181E+02	DMARG=	.2365E+02	A=	.1444E-01
2	FWR=	.1469E+02	OMARG=	.9274E+01	DMARG=	.2365E+02	A=	.2258E-03
1	FWR=	.2574E+01	OMARG=	.1075E+02	DMARG=	.2365E+02	A=	.7276E+00
2	FWR=	.2609E+02	OMARG=	.3107E+02	DMARG=	.2365E+02	A=	.1285E-02
1	FWR=	.3197E+01	OMARG=	.1935E+02	DMARG=	.2365E+02	A=	.2461E+00
2	FWR=	.1981E+02	OMARG=	.2311E+02	DMARG=	.2365E+02	A=	.1318E-02
1	FWR=	.7068E+01	OMARG=	.2449E+02	DMARG=	.2365E+02	A=	.3302E+00
2	FWR=	.2014E+02	OMARG=	.2027E+02	DMARG=	.2365E+02	A=	.1318E-02
1	FWR=	.6361E+01	OMARG=	.2282E+02	DMARG=	.2365E+02	A=	.5969E+00
2	FWR=	.2145E+02	OMARG=	.5249E+02	DMARG=	.2365E+02	A=	.7479E-03
1	FWR=	.6691E+01	OMARG=	.2286E+02	DMARG=	.2365E+02	A=	.2637E-01
2	FWR=	.2223E+02	OMARG=	.2303E+02	DMARG=	.2365E+02	A=	.3270E-03
1	FWR=	.1082E+02	OMARG=	.2909E+02	DMARG=	.2365E+02	A=	.4241E+00
2	FWR=	.2307E+02	OMARG=	.1824E+02	DMARG=	.2365E+02	A=	.3270E-03
1	FWR=	.7099E+01	OMARG=	.2069E+02	DMARG=	.2365E+02	A=	.5079E+00
2	FWR=	.2596E+02	OMARG=	.2697E+02	DMARG=	.2365E+02	A=	.8555E-03
1	FWR=	.7975E+01	OMARG=	.2318E+02	DMARG=	.2365E+02	A=	.4040E+00
2	FWR=	.2441E+02	OMARG=	.2418E+02	DMARG=	.2365E+02	A=	.7579E-03
1	FWR=	.8174E+01	OMARG=	.2368E+02	DMARG=	.2365E+02	A=	.4361E+00
2	FWR=	.2416E+02	OMARG=	.2364E+02	DMARG=	.2365E+02	A=	.7689E-03
1	FWR=	.8370E+01	OMARG=	.2379E+02	DMARG=	.2414E+02	A=	.9915E-01
2	FWR=	.2439E+02	OMARG=	.2368E+02	DMARG=	.2414E+02	A=	.5678E-04
1	FWR=	.8975E+01	OMARG=	.2268E+02	DMARG=	.2414E+02	A=	.9915E-01
2	FWR=	.2654E+02	OMARG=	.2567E+02	DMARG=	.2414E+02	A=	.2957E-03
1	FWR=	.1068E+02	OMARG=	.2720E+02	DMARG=	.2414E+02	A=	.4563E+00
2	FWR=	.2489E+02	OMARG=	.2094E+02	DMARG=	.2414E+02	A=	.6592E-03
1	FWR=	.9405E+01	OMARG=	.2402E+02	DMARG=	.2414E+02	A=	.4684E+00
2	FWR=	.2587E+02	OMARG=	.2424E+02	DMARG=	.2414E+02	A=	.6878E-03
1	FWR=	.9523E+01	OMARG=	.2415E+02	DMARG=	.2439E+02	A=	.1620E+00
2	FWR=	.2593E+02	OMARG=	.2415E+02	DMARG=	.2439E+02	A=	.6878E-03
1	FWR=	.9739E+01	OMARG=	.2441E+02	DMARG=	.2439E+02	A=	.1767E+00
2	FWR=	.2602E+02	OMARG=	.2396E+02	DMARG=	.2439E+02	A=	.6878E-03
1	FWR=	.9721E+01	OMARG=	.2422E+02	DMARG=	.2439E+02	A=	.1555E+01
2	FWR=	.2617E+02	OMARG=	.2420E+02	DMARG=	.2439E+02	A=	.3684E-03
1	FWR=	.9749E+01	OMARG=	.2404E+02	DMARG=	.2451E+02	A=	.1555E+01
2	FWR=	.2638E+02	OMARG=	.2444E+02	DMARG=	.2451E+02	A=	.2881E-03
1	FWR=	.9792E+01	OMARG=	.2405E+02	DMARG=	.2451E+02	A=	.2707E-01
2	FWR=	.2643E+02	OMARG=	.2446E+02	DMARG=	.2451E+02	A=	.7159E-04
1	FWR=	.1172E+02	OMARG=	.2727E+02	DMARG=	.2451E+02	A=	.2669E+00
2	FWR=	.2660E+02	OMARG=	.2161E+02	DMARG=	.2451E+02	A=	.7159E-04
1	FWR=	.1003E+02	OMARG=	.2299E+02	DMARG=	.2451E+02	A=	.3552E+00
2	FWR=	.2770E+02	OMARG=	.2589E+02	DMARG=	.2451E+02	A=	.7031E-03
1	FWR=	.1052E+02	OMARG=	.2430E+02	DMARG=	.2451E+02	A=	.2995E+00
2	FWR=	.2726E+02	OMARG=	.2456E+02	DMARG=	.2451E+02	A=	.6791E-03
1	FWR=	.1060E+02	OMARG=	.2447E+02	DMARG=	.2451E+02	A=	.2358E+00
2	FWR=	.2724E+02	OMARG=	.2441E+02	DMARG=	.2451E+02	A=	.1850E-02

6.144 CP SECONDS EXECUTION TIME.

Fig. 5.2 Illustration of Margin Leveling Progression

of option one (see fig. 5.1), the margins would be leveled at this point with the leveled margins being the obtained margins at convergence.

Since option one is chosen, the desired margins are decremented by half of the largest difference between the desired and the obtained margins. This difference occurs at the second link and is 1.97 db. At the end of the second convergence the second link is still at maximum uplink power so the desired margins are again decremented but only by half of the prior decrement. On the next convergence, the new margins are achieved for both links so the desired margins are increased by half of the prior decrement. This procedure continues until the decrement or increment is less than 0.1 db.

At the end of the last convergence it is noted that the uplink power for the second link is within 0.5 db of the maximum power. This difference can be made smaller by decreasing the minimum delta required for margin leveling. Theoretically, there should be at least one uplink power at its maximum for margin leveling to occur.

In tables 5.1 and 5.2, the results of margin leveling for the simple two link system is shown with option zero and option one chosen, respectively. The maximum EIRP for the first and second link is 94.0 and 69.0 db, respectively. It is seen that the leveled margins for the two options are quite different. For the case with all margins leveled, table 5.2, the value of the leveled margins, 24.5 db, lie between the leveled margins for the case where only the unachievable margins are leveled, as is expected.

Table 5.1

Margin Leveling Results for a Two Link System
Option 0 Selected

Link Number	Uplink EIRP (dbw)	Leveled Margin (db)	Desired Margin (db)
1	72.1	26.6	26.6
2	69.0	22.7	26.6

Table 5.2

Margin Leveling Results for a Two Link System
Option 1 Selected

Link Number	Uplink EIRP (dbw)	Leveled Margin (db)	Desired Margin (db)
1	70.6	24.5	26.6
2	68.5	24.4	26.6

As seen in this chapter, the margin leveling algorithm performed quite well for a simple two link system. In the next chapter, the algorithm's performance is discussed when applied to larger systems.

VI. Performance and Results of Margin Leveling Algorithm

In chapter five, the margin leveling algorithm itself was introduced and discussed. In this chapter, the performance of the algorithm is discussed and some leveled margins are shown for systems involving up to twenty links. More specifically, the CPU time required for the algorithm to complete margin leveling is discussed with the number of links and the difference between the desired and the leveled margins as parameters.

Margin Leveling Results

In chapter five, the margin leveling results were shown for a simple two link system. In table 6.1 and 6.2, the leveled margins are shown for a sixteen link system with no two links being identical. Table 6.1 shows the leveled margins for the case where only the margins of the unachievable links are leveled and table 6.2 shows the results where all margins are leveled until the difference between the desired and the leveled margins are minimized. The specific link configurations used are shown in table 6.3.

The uplink and downlink frequencies used are 7.99 GHz and 7.3 GHz, respectively. The bandwidth of the CDMA signals is 50 MHz and the transmit power of the satellite is 40 watts. The satellite receiving and transmitting antennas each have a gain of 16.8 db with a front end noise temperature of 1514 °K.

Table 6.6

Predicted CPU Time to Perform Margin Leveling
(CYBER computer)

Number of Links	CPU Time (sec)	
	Option 0	Option 1
5	13.4	99.7
10	64.4	412.2
20	310.3	1,704.1
40	1,494.7	7,044.9
60	3,749.1	16,159.9
80	7,199.3	29,124.9
100	11,942.1	45,993.5

As seen from the previous figures and tables, the amount of computation time required to perform margin leveling increases quite rapidly as the number of links accessing a satellite increases. In order to utilize the margin leveling algorithm for a large number of links, some modification of the algorithm will be needed to increase its efficiency. In the following chapter some recommendations are given as to how this may be accomplished.

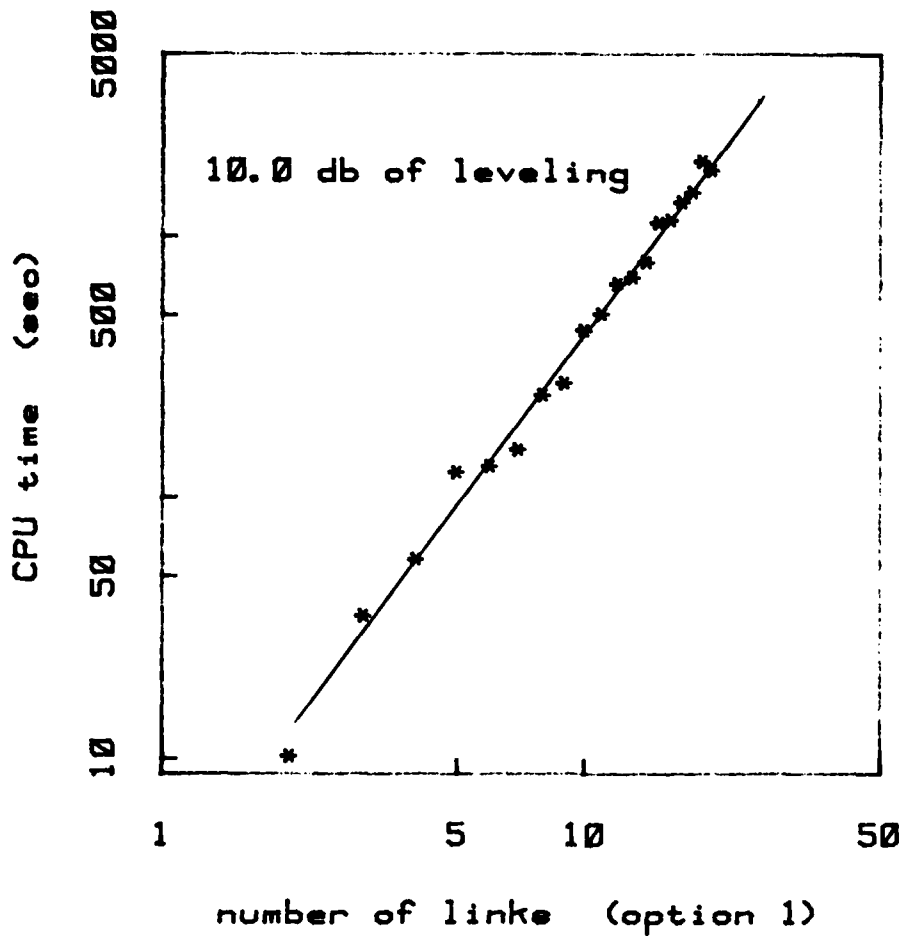


Fig. 6.8 CPU Time Versus Number of Links (Logrithmic)

results of Eqs (6.2) and (6.3) for a various number of links. As the number of links increases by a factor of 10, the required CPU time increases by a factor of 185.4 and 111.4 for option zero and option one, respectively.

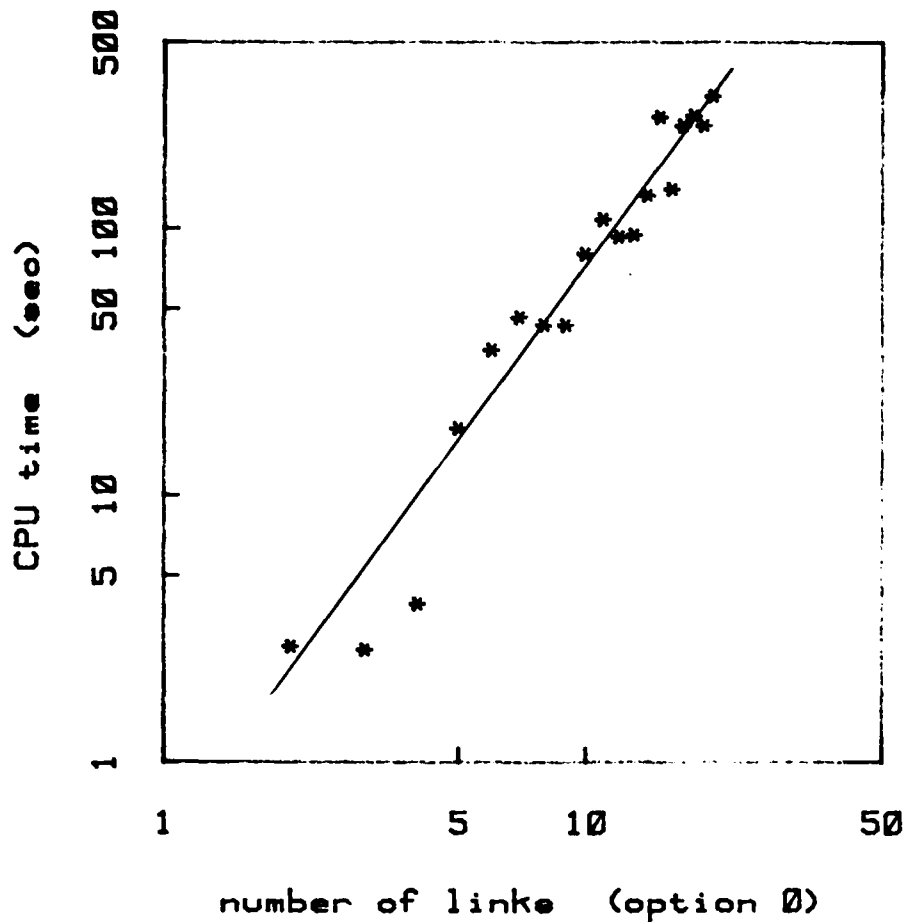


Fig. 6.7 CPU Time Versus Number of Links (Logarithmic)

$$\text{CPU time} = 3.694(\text{number of links})^{2.0467} \quad (6.3)$$

Equations (6.2) and (6.3) are dependent on the computer system utilized, but the general equation of Eq (6.1) should still hold regardless of the system as long as the algorithm is unchanged.

The predicted CPU time to perform margin leveling on any number of links can now be found for either option. Table 6.6 shows the

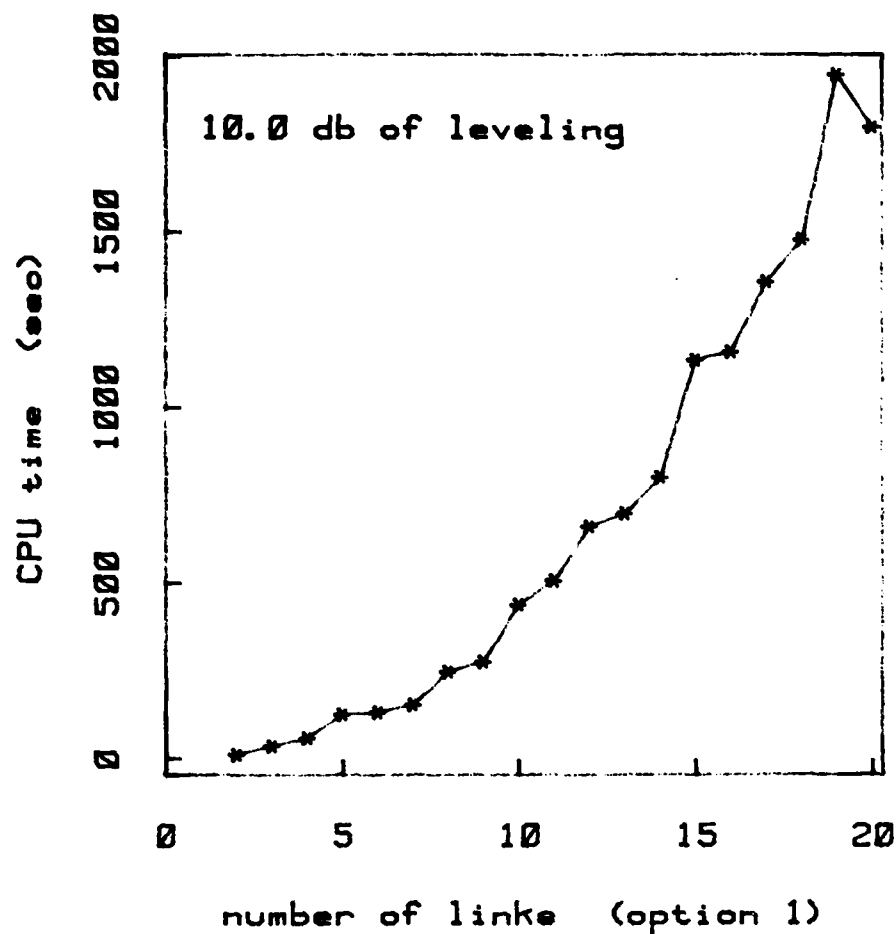


Fig. 6.6 CPU Time Versus Number of Links

For the case where margin leveling is performed only on the links with unachievable margins, the power relationship is found to be

$$\text{CPU time} \approx 0.3476(\text{number of links})^{2.268} \quad (6.2)$$

For the case of total margin leveling, the power relationship is found to be

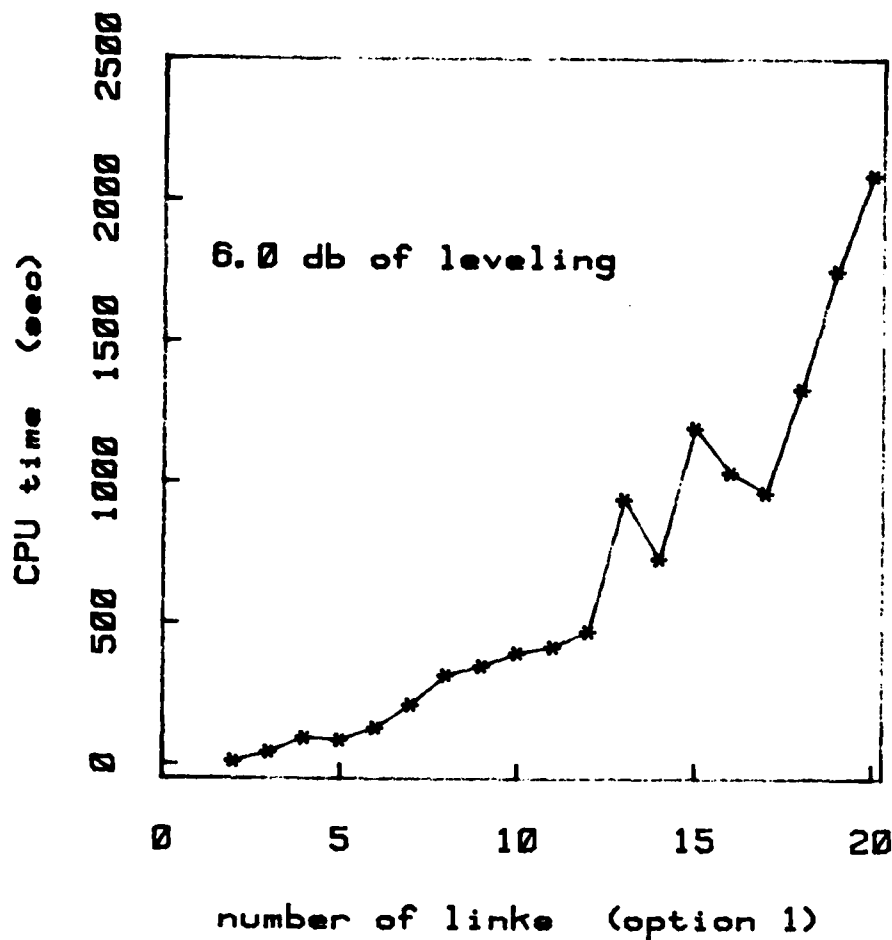


Fig. 6.5. CPU Time Versus Number of Links

$$\text{CPU time} = a(\text{number of links})^b \quad (6.1)$$

where a and b are to be determined.

Two relationships are determined with the aid of the logarithmic graphs of figure (6.7) and (6.8) corresponding to figures (6.1) and (6.6), respectively. Since the logarithmic graphs are approximately linear, the power relations must hold.

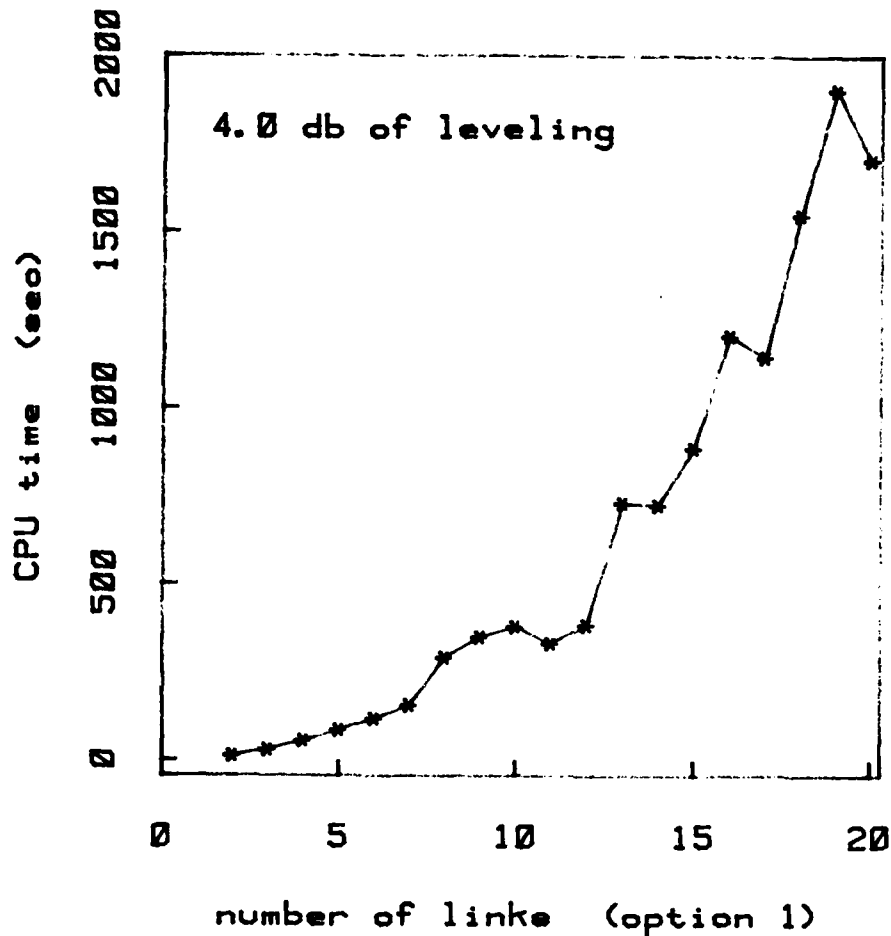


Fig. 6.4. CPU Time Versus Number of Links

10 db case is less than that of the 1 db case. Thus the time to achieve margin leveling for the 10 db case may be less than that of the 1 db case.

Although the graphs do not show any correlation between the amount of margin leveling achieved and the CPU time required for margin leveling, they do show a general trend of an increase in CPU time required as the number of links increase. The trend can be shown to be a power relationship of the form

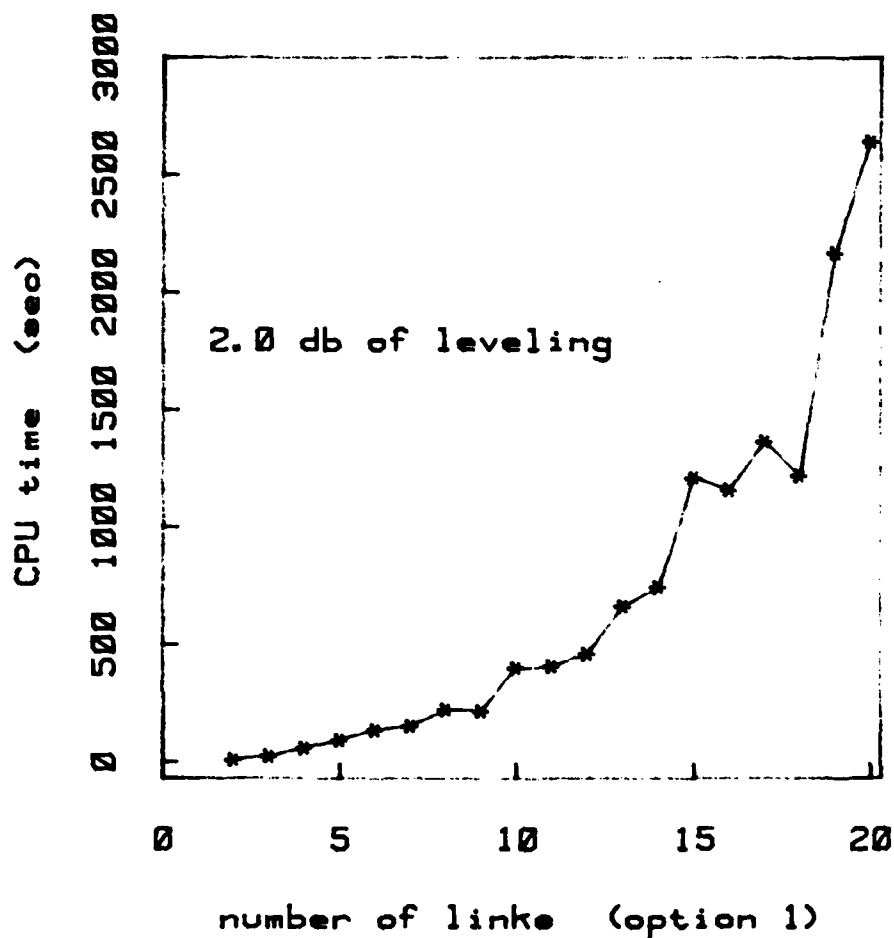


Fig. 6.3. CPU Time Versus Number of Links

had to pass through the convergence routine turned out to be 7 and that of the 10 db of leveled margin case turned out to be 9. Thus, the 20 db of leveled margin case passed through the convergence routine 2 more times than the 1 db case. Even though the 10 db case requires two more passes through the convergence routine, the amount of time spent in a specific convergence routine varies. It may be the case that the average time spent in a convergence routine for the

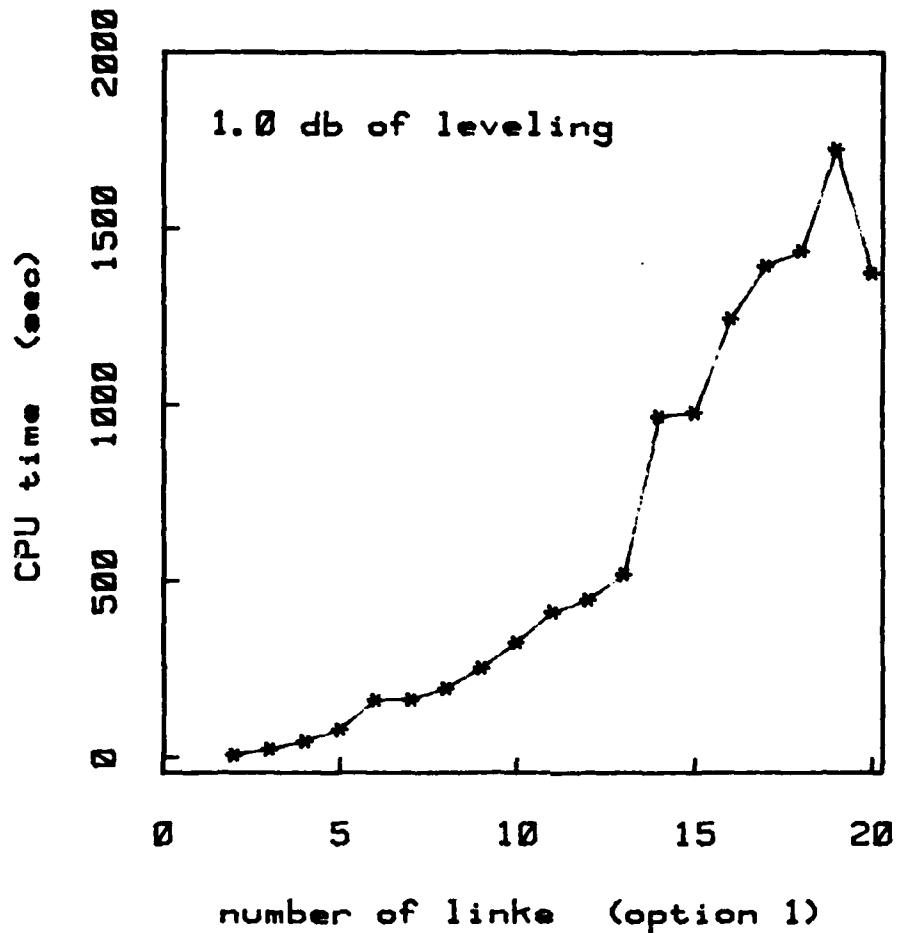


Fig. 6.2 CPU Time Versus Number of Links

To help understand the above results, a seventeen link system with a margin leveling of 1 db and 10 db was analyzed. The initial difference between the desired and obtained margins after the first convergence turned out to be 7.8 db and 27.3 db for the 1 db and 10 db of margin leveling, respectively. To achieve margin leveling, the initial difference is to be halved until the difference is below 0.1 db. The number of times in which the 1 db of leveled margin case

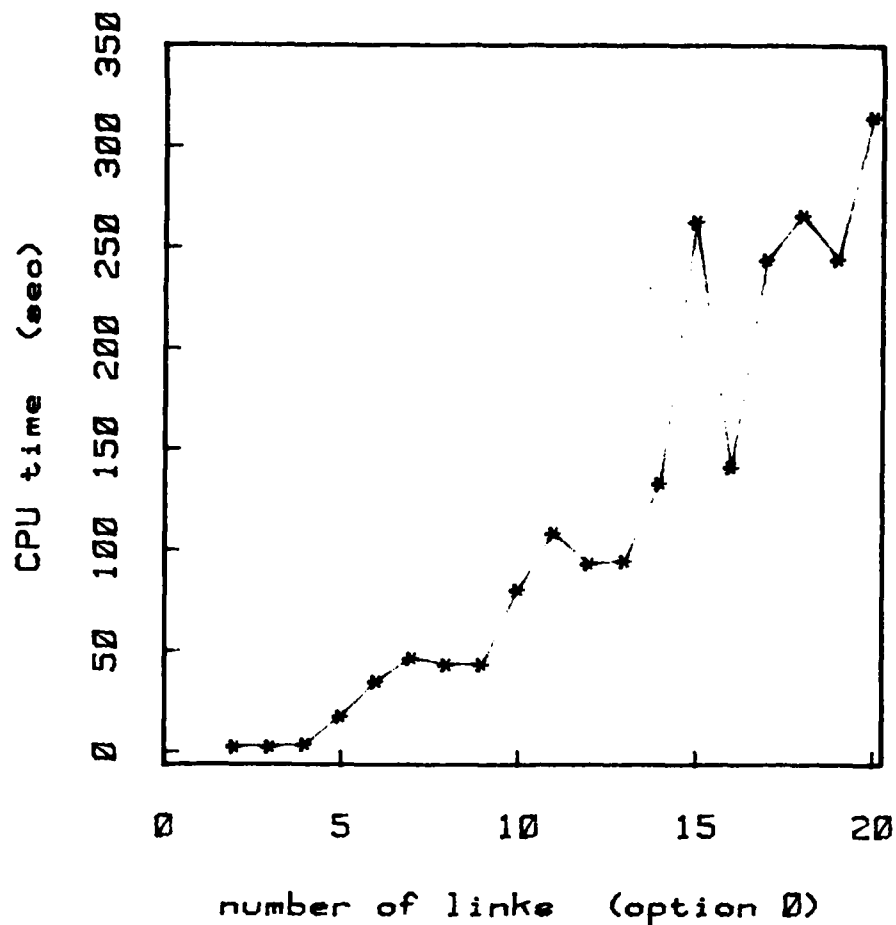


Fig. 6.1 CPU Time Versus Number of Links

greater as the desired margins become greater. This initial difference is continually halved and used to create new margins until the difference becomes less than 0.1 db. At this point the margins are considered leveled and the routine stops. It would therefore seem that the algorithm would require more time to level margins when the initial difference between the leveled and obtained margins is greater.

Table 6.5

Specific Link Configurations with Respect to
the Number of Links

Number of Links	Number of Specific Configuration Used				
	1	2	3	4	5
2	1	0	0	0	1
3	1	0	1	0	1
4	1	0	1	1	1
5	1	1	1	1	1
6	1	1	1	1	2
7	1	1	1	2	2
8	1	1	2	2	2
9	1	2	2	2	2
10	2	2	2	2	2
11	2	2	2	2	3
12	2	2	2	3	3
13	2	2	3	3	3
14	2	3	3	3	3
15	3	3	3	3	3
16	3	3	3	3	4
17	3	3	3	4	4
18	3	3	4	4	4
19	3	4	4	4	4
20	4	4	4	4	4

Figure 6.1 shows how the CPU time is affected by an increase in the number of links for the case where only the links with unachievable margins are leveled. Figures (6.2) through (6.6) show graphs of CPU time versus the number of links for different values of margin leveling with all margins leveled. Figure 6.2 shows the graph of CPU time versus number of links with 1.0 db of margin leveling and figure (6.6) shows a similar graph for a margin leveling of 10.0 db.

As shown by the graphs, the amount of margin leveling does not seem to affect the length of time needed to obtain the margins. This result was unexpected since the largest difference between the desired margin and the obtained margin, after the first convergence, becomes

more than 10 links was on the order of hundreds of CPU minutes on a VAX 11/780 computer. In a time sharing environment the hundred minutes of CPU time required about 24 hours of real time depending on the system load. Since this delay could not be accepted, a faster machine was utilized. With the use of a CYBER computer system the required CPU time was decreased by a factor of five or so. With the CYBER, results could be expected within hours instead of days. However, even with the use of a CYBER, the allotted CPU time per job of approximately 2000 CPU seconds was still exceeded when trying to level the margins of more than twenty links.

To study the effects of the amount of CPU time required to level the margins of many links, five link configurations were used as shown in table 6.4. The specific combinations of the five links is shown in table 6.5 for each of the 19 sets of links ranging in number from 2 to 20.

Table 6.4
Link Configurations Used to Evaluate Required
CPU Time vs. Number of Links

Link Configuration	Maximum uplink EIRP (dbw)	Receiver Antenna Gain (db)	Receiver Noise Temp ($^{\circ}$ K)	Data Rate (b/s)	E_b/N_o (db)
1	94.0	60.0	125.0	32000	9.0
2	89.0	60.0	158.0	16000	9.0
3	79.0	50.6	288.0	9600	9.0
4	73.0	42.6	288.4	3000	9.0
5	69.0	41.3	339.0	2400	9.0

leveled margin and the desired margin is approximately 0.5 db for each link. Therefore, if 0.5 db of margin can be sacrificed for each link, then all 16 links can remain in operation whereas with the configuration given in table 6.1, some links may have to be taken off the system. It is also interesting to note that the average leveled margin in table 6.2 is approximately 1.0 db higher than the average leveled margin of table 6.1. The significance of this fact is not evident until the average uplink power is calculated. It is seen that the average uplink power in table 6.2 is lower than that of table 6.1 by approximately 5.0 db per link. Therefore, for this specific 16 link set, a decrease in the average uplink power causes an increase in the average leveled margin.

The above phenomena may be due to the amount of intermodulation produced in the band-pass limiter and TWTA. It seems that when there is a large difference between the amplitude of the incoming signals, more intermodulation distortion is produced than if the signals were of an equal level. For the leveling of only the unachievable margins this difference is about 11.5 db (links 6,16). As additional modulation distortion is produced, the power available for undistorted signal output decreases. Therefore, additional uplink power is required to achieve a specific set of margins when the modulation distortion has increased.

CPU Time Constraints

During the initial stages of coding and execution of the margin leveling algorithm it was found that the required CPU time to level

From tables 6.1 through 6.3, it is seen that link number thirteen is the link which limits the system. In table 6.1, it is seen that this link has the largest difference between the leveled and desired margins. In table 6.2, this link is the link which is driven closest to its maximum uplink power. Both of these results are expected as seen in table 6.3 where the data rate and desired margin are both high for that type of link (fairly low EIRP).

Table 6.3

Link Configuration for 16 Link Nonhomogeneous System

Link Number	Maximum uplink EIRP (dbw)	Receiver Antenna Gain (db)	Receiver Noise Temp ($^{\circ}$ K)	Data Rate (b/s)	E_b/N_o (db)	Desired Margin (db)
1	94.0	60.0	125.0	32000	9.0	16.0
2	94.0	50.6	288.0	15200	9.0	16.0
3	94.0	41.3	339.0	12000	9.0	14.0
4	89.0	60.0	158.0	16000	9.0	17.0
5	89.0	50.6	288.0	16000	9.0	16.0
6	89.0	42.6	288.4	19200	9.0	15.0
7	79.0	60.0	125.0	19200	9.0	16.0
8	79.0	50.6	288.0	9600	9.0	17.0
9	79.0	41.3	339.0	9600	9.0	15.0
10	73.0	60.0	125.0	9600	9.0	15.0
11	73.0	50.6	288.0	9600	9.0	15.0
12	73.0	41.3	339.0	4800	9.0	13.0
13	69.0	60.0	125.0	12000	9.0	16.0
14	69.0	60.0	158.0	9600	9.0	16.0
15	69.0	42.6	288.4	3600	9.0	15.0
16	69.0	41.3	339.0	2400	9.0	15.0

From tables 6.1 and 6.2, it is clear that the algorithm performs quite well for a nonhomogeneous link scenario. In table 6.1, the first nine links have achieved their desired margins while the remaining links have not. Thus, the last seven links are operating at maximum uplink power. In table 6.2, the difference between the

Table 6.1

Margin Leveling Results for Nonhomogeneous 16 Link System
Option 0

Link Number	Uplink EIRP (dbw)	Leveled Margin (db)	Desired Margin (db)
1	79.4	16.2	16.0
2	77.4	16.1	16.0
3	79.1	14.2	14.0
4	77.6	17.1	17.0
5	77.6	16.2	16.0
6	80.6	15.2	15.0
7	77.3	16.0	16.0
8	76.5	17.1	17.0
9	79.0	15.0	15.0
10	73.0	14.6	15.0
11	73.0	13.5	15.0
12	73.0	11.7	13.0
13	69.0	9.5	16.0
14	69.0	10.5	16.0
15	69.0	10.3	15.0
16	69.0	10.6	15.0

Table 6.2

Margin Leveling Results for Nonhomogeneous 16 Link System
Option 1

Link Number	Uplink EIRP (dbw)	Leveled Margin (db)	Desired Margin (db)
1	72.3	15.5	16.0
2	70.2	15.5	16.0
3	71.9	13.5	14.0
4	70.4	16.5	17.0
5	70.4	15.4	16.0
6	73.2	14.2	15.0
7	70.2	15.5	16.0
8	69.3	16.5	17.0
9	71.9	14.5	15.0
10	66.3	14.4	15.0
11	67.3	14.4	15.0
12	67.1	12.4	13.0
13	68.3	15.5	16.0
14	67.3	15.4	16.0
15	66.5	14.5	15.0
16	66.2	14.5	15.0

VII. Recommendations and Conclusions

As seen in chapter 6, the major limitation of the margin leveling algorithm is the CPU time required to perform margin leveling for a large number of links. In this chapter some recommendations are given that may increase the speed of the algorithm.

Integration Speed

The underlying cause of the large CPU times required by the leveling algorithm is the complexity of the integrals in Eqs (3.39) and (3.41). The integration is performed twice in the margin leveling algorithm for each link, once for the band-pass limiter and again for the saturated TWTA. It may be possible to perform the integration once and then square the result to get the TWTA output. The limiting value of the hard limiter for the single integration would have to be the square root of the TWTA limiting value to get the desired magnitude of TWTA output. The squaring of a single integration for a one link system yields approximately the same results as performing two integrations, as seen in figure (2.7). It is not known if this result is true for a system with more than one link, but if so, the required CPU time for margin leveling would be decreased by a factor of two.

Another method of reducing the CPU time would be to simplify the integral mentioned above particularly when a large number of links are involved. As the number of links increase, the integrand, consisting of a product of bessel functions, tends to decrease by the reciprocal

of the square root of the argument for each link added (6:490). It may be possible to use a polynomial expansion of the Bessel functions neglecting the higher order terms. With this method there may even be an analytical solution to the integral, but it seems unlikely. The accuracy of the polynomial expansion would have to be evaluated by comparison of the results obtained.

The integration time may be decreased even further if a more efficient integration routine is used. In the present algorithm, the integration is performed by an International Mathematical and Statistical Library (IMSL) routine, DCADRE, which utilizes a cautious adaptive Romberg extrapolation integration technique (7:DCADRE-1). There may be more efficient methods for integrating the desired function. The reason for the use of DCADRE was mainly that of convenience, i.e. it was readily available.

Additional Recommendations for Decreasing CPU Time

Up to this point, the recommendations for decreasing the required CPU time for margin leveling involves the integration which takes place in the algorithm. It may also be possible to decrease the CPU time by making changes to the leveling algorithm itself.

In the present algorithm, after some links have reached maximum uplink power and the others have obtained the desired margins, margin leveling is performed by decrementing the desired margins by half of the largest difference between the desired and the obtained margins. It may be advantageous to decrement the margins by the difference between the averages of the obtained and desired margins. It seems

that this method would cause quicker leveling and it should be investigated.

The final and possibly the simplest method to decrease CPU time is to use a faster computer. This method, however, is more expensive than the others.

Of the above recommendations, it is felt that the implimentation of two of the suggestions would have a significant effect on the CPU time whereas the others would have only minimal effect. The two recommendations are listed again in order of expected benefit in decreased CPU time.

1. Utilize the difference between the average of the obtained and desired margin to perform margin leveling.
2. Attempt to square the integral of Eq (3.39) instead of performing both integrals of Eqs (3.23) and (3.39).

Further Study

The recommendations made so far deal only with small modifications to the existing algorithm. In order to better model a CDMA satellite system, it is necessary to include more than one link per terminal or antenna. In actuality there is more than one link on each earth terminal. Therefore, instead of dealing with one uplink power which cannot exceed a maximum, it is necessary to deal with a sum of uplink powers where the entire sum cannot exceed a maximum.

The above scenario adds another dimension to the problem. Instead of just power sharing in the satellite, there is also power

sharing at the earth terminal. When the terminal power is at its maximum, the individual uplink powers can still be changed, but an increase in one uplink power must be brought about by a decrease in some other uplink powers for that terminal.

The algorithm for the above scenario would be quite similar to the present algorithm with the only difference being in the use of a maximum terminal power instead of a maximum uplink power. Instead of testing an individual link for its maximum power, a sum of specific uplink powers should be tested against a maximum uplink terminal power.

Conclusions

The goal of this thesis was to develop an algorithm which performed margin leveling on an arbitrary number of links accessing a satellite with a hard limiting transponder where code division multiple access communications was used as the signalling scheme. The desired algorithm was required to perform two types of margin leveling; the first being the leveling of only the margins not achieving their respective desired margins, and the second being the leveling of all margins. In either case, the difference between the desired and the leveled margin was to be minimized.

The designed margin leveling algorithm performed quite well in that the margins were properly leveled with respect to the option selected by the user. However, the computer execution time required to obtain the leveled margins was quite high and increased proportionally to the square of the number of links.

A significant decrease in the required CPU time may be achieved if the two recommendations given in chapter seven are followed.

Appendix A: Correlation Analysis of Nonlinear Devices

Throughout chapter two and three of this thesis the output auto correlation for a hard limiter were utilized in Eqs (2.27) and (3.13). These equations are derived in this appendix using correlation analysis for nonlinear devices.

Single Carrier Correlation Analysis

For nonlinear devices, the output, $y(t)$, can be written as

$$y(t) = g(x(t)) \quad (A.1)$$

where $x(t)$ is the input into the nonlinear device. The fourier transform of $y(t)$ is then written as

$$F(y(t)) = F(g(x(t))) = G(\omega) = \int_{-\infty}^{\infty} g(x(t))e^{-j\omega x(t)} dx \quad (A.2)$$

The output of the nonlinear device can now be written as an inverse fourier transform

$$y(t) = F^{-1}(G(\omega)) = (1/2\pi) \int_{-\infty}^{\infty} G(\omega)e^{j\omega x(t)} d\omega \quad (A.3)$$

The output auto correlation, $R_y(\tau)$, can now be written as

$$R_y(\tau) = E(y(t)y(t + \tau))$$

$$= (1/2\pi)^2 \int_{-\infty}^{\infty} \int_{-\infty}^{\infty} G(\omega_1)G(\omega_2)\psi_x(\omega_1, \omega_2, \tau) d\omega_1 d\omega_2 \quad (A.4)$$

where

$$\psi_x(\omega_1, \omega_2, \tau) = E[e^{j\omega_1 x(t)} e^{j\omega_2 x(t + \tau)}]$$

If $x(t)$ is a sum of a modulated carrier, $a(t)\cos(\omega_c t + \theta(t))$, plus zero mean, independent, bandpass, additive white gaussian noise, $n(t)$, then $\psi_x(\omega_1, \omega_2, \tau)$ can be written as

$$\psi_x(\omega_1, \omega_2, \tau) = \psi_s(\omega_1, \omega_2, \tau)\psi_n(\omega_1, \omega_2, \tau) \quad (A.5)$$

where

$$\psi_s(\omega_1, \omega_2, \tau) = E[e^{j\omega_1 a(t)\cos(\omega_c t + \theta(t))} e^{j\omega_2 a(t+\tau)\cos[\omega_c(t+\tau) + \theta(t+\tau)]}] \quad (A.6)$$

$$\psi_n(\omega_1, \omega_2, \tau) = E[e^{j\omega_1 n(t)} e^{j\omega_2 n(t+\tau)}] \quad (A.7)$$

Using the Jacobi-Anger identity (2:1078) given below

$$e^{z\cos\phi} = \sum_{n=0}^{\infty} \epsilon_n I_n(z) \cos n\phi \quad (A.8)$$

where

$$\epsilon_n = \begin{cases} 1, & n = 0 \\ 2, & n = 1, 2, 3, \dots \end{cases}$$

and $I_n(z)$ is the modified bessel function, $\psi_s(\omega_1, \omega_2, \tau)$ can then be

written as the double summation

$$\psi_s(\omega_1, \omega_2, \tau) = \sum_{i=0}^{\infty} \sum_{k=0}^{\infty} \epsilon_i \epsilon_k E[I_1(j\omega_1 a(t)) I_k(j\omega_2 a(t+\tau))] R_c(\tau, i, k) \quad (A.9)$$

where

$$R_c(\tau, i, k) = E[\cos(i(\omega_c t + \theta(t))) \cos(k(\omega_c (t+\tau) + \theta(t+\tau)))] \quad (A.10)$$

Expanding $R_c(\tau, i, k)$ yields

$$R_c(\tau, i, k) = \frac{1}{2} E[\cos((i-k)\omega_c t - k\omega_c \tau + i\theta(t) - k\theta(t+\tau)) + \cos((i+k)\omega_c t + k\omega_c \tau + i\theta(t) + k\theta(t+\tau))] \quad (A.11)$$

For phase modulation where $\theta(t)$ is uniformly distributed over 0 to 2π or for phase shift keyed signalling with equiprobable phases, $R_c(\tau, i, k)$ can be simplified to

$$R_c(\tau, i, k) = \begin{cases} 1 & , i=k=0 \\ \frac{1}{2} \cos(i(\omega_c \tau - \theta(t) + \theta(t+\tau))) & , i=k \neq 0 \\ 0 & , i \neq k \end{cases} \quad (A.12)$$

and can be written as

$$R_c(\tau, i, k) = \begin{cases} (1/\epsilon_1) \cos(i(\omega_c \tau - \theta(t) + \theta(t+\tau))) & , i=k \\ 0 & , i \neq k \end{cases} \quad (A.13)$$

From Eqs (A.13) and (A.9), $\psi_s(\omega_1, \omega_2, \tau)$ can be simplified for phase shift keyed signalling where $a(t)=A$, to form

$$\psi_s(\omega_1, \omega_2, \tau) = \sum_{i=0}^{\infty} \epsilon_i [I_1(j\omega_1 A) I_1(j\omega_2 A)] \cos(i(\omega_c \tau - \theta(t) + \theta(t+\tau))) \quad (A.14)$$

The noise term of Eq (A.7) can now be analyzed. The joint characteristic function for zero mean gaussian noise is known to be (4:225,476)

$$E[e^{j\omega_1 n(t)} e^{j\omega_2 n(t+\tau)}] = \psi_n(\omega_1, \omega_2, \tau) = e^{-(\omega_1^2 + \omega_2^2)R_n(0)/2} e^{-j\omega_1 \omega_2 R_n(\tau)} \quad (A.15)$$

Using the infinite series expansion for $e^{-R_n(\tau)\omega_1\omega_2}$, $\psi_n(\omega_1, \omega_2, \tau)$ can be written as

$$\psi_n(\omega_1, \omega_2, \tau) = e^{-(\omega_1^2 + \omega_2^2)R_n(0)/2} \sum_{i=0}^{\infty} \frac{(-1)^i R_n^i(\tau) \omega_1^i \omega_2^i}{i!} \quad (A.16)$$

Combining Eqs (A.16) and (A.14) to form $\psi_x(\omega_1, \omega_2, \tau)$ and substituting $\psi_x(\omega_1, \omega_2, \tau)$ into Eq (A.4) gives the output autocorrelation of a nonlinear device with an input consisting of a phase modulated sinusoid plus narrow band gaussian noise.

$$R_y(\tau) = (1/2\pi)^2 \int_{-\infty}^{\infty} \int_{-\infty}^{\infty} G(\omega_1) G(\omega_2) \sum_{i=0}^{\infty} \sum_{k=0}^{\infty} \epsilon_i I_i(j\omega_1 A) I_i(j\omega_2 A) e^{-\omega_1^2 R_n(0)/2} \\ \times e^{-\omega_2^2 R_n(\tau)/2} ((-1)^k R_n^k(\tau) \omega_1^k \omega_2^k / k!) \cos(i(\omega_c \tau - \theta(t) + \theta(t+\tau))) d\omega_1 d\omega_2 \quad (A.17)$$

If h_{ik} is defined as

$$h_{ik} = (1/2\pi) \int_{-\infty}^{\infty} G(\omega) \omega^k I_1(j\omega A) e^{-R_n(0)\omega^2/2} d\omega \quad (A.18)$$

then $R_y(\tau)$ can be written as

$$R_y(\tau) = \sum_{i=0}^{\infty} \sum_{k=0}^{\infty} (-1)^k (\epsilon_1/k!) h_{ik}^2 R_n^k(\tau) \cos(i(\omega_c \tau - \theta(t) + \theta(t+\tau))) \quad (A.19)$$

The carrier power can now be found by letting $\tau=0$, $i=1$, and $k=0$ since the summation over i is due to the signal and the summation over k is due to the noise. Therefore, the output signal power, P_{so} , at the frequency of the input can be written as

$$P_{so} = 2h_{10}^2 = (2/(2\pi)^2) \left[\int_{-\infty}^{\infty} G(\omega) I_1(j\omega A) e^{-R_n(0)\omega^2/2} d\omega \right]^2 \quad (A.20)$$

From the fact that $I_n(j\omega A) = j^n J_n(\omega A)$, P_{so} can be simplified to

$$P_{so} = 2 \left[(1/2\pi) \int_{-\infty}^{\infty} jG(\omega) J_1(\omega A) e^{-R_n(0)\omega^2/2} d\omega \right]^2 \quad (A.21)$$

Multiple Carrier Correlation Analysis

In chapter 3, the output autocorrelation for a multiple carrier input into a non-linear device is shown in Eq (3.13). This section of the appendix deals with the derivation of this equation.

The total input of M phase modulated signals into the nonlinear device is written as

$$x(t) = \sum_{i=1}^M a_i \cos(\omega_c t + \theta_i(t)) \quad (A.22)$$

The second order characteristic function of the signal, Eq (A.6), can be written as

$$\begin{aligned} \psi_s(\omega_1, \omega_2, \tau) &= E[\exp(j\omega_1 \sum_{i=1}^M a_i \cos(\omega_c t + \theta_i(t))) \\ &\quad \times \exp(j\omega_2 \sum_{i=1}^M a_i \cos(\omega_c (t + \tau) + \theta_i(t + \tau)))] \end{aligned} \quad (A.23)$$

and with the use of the Jacobi-Anger identity, Eq (A.8), $\psi_s(\omega_1, \omega_2, \tau)$ can be written as

$$\psi_s(\omega_1, \omega_2, \tau) = \prod_{i=1}^M \sum_{m=0}^{\infty} \sum_{n=0}^{\infty} \epsilon_m \epsilon_n I_m(j\omega_1 a_i) I_n(j\omega_2 a_i) R_c(i, m, n, \tau) \quad (A.24)$$

where

$$R_c(i, m, n, \tau) = E[\cos(m(\omega_c t + \theta_i(t))) \cos(n(\omega_c (t + \tau) + \theta_i(t + \tau)))] \quad (A.25)$$

If the phase distribution is uniform, then $R_c(i, m, n, \tau)$ can be simplified to a form similar to Eq (A.13). The simplification yields

$$R_c(i, m, n, \tau) = \begin{cases} (1/\epsilon_n) \cos(\omega_c \tau - \theta_i(t) + \theta_i(t + \tau)) & n=m \\ 0 & n \neq m \end{cases}$$

With this simplification, the characteristic function is rewritten as

$$\psi_s(\omega_1, \omega_2, \tau) = \prod_{i=1}^M \sum_{m=0}^{\infty} \epsilon_m I_{m_1}(j\omega_1 a_1) I_{m_1}(j\omega_2 a_1) \cos(\omega_c \tau - \theta_1(t) + \theta_1(t+\tau)) \quad (A.26)$$

This characteristic function is a product of M infinite series and can be expanded as shown here.

$$\begin{aligned} \psi_s(\omega_1, \omega_2, \tau) = & \sum_{m_1=0}^{\infty} \epsilon_{m_1} I_{m_1}(j\omega_1 a_1) I_{m_1}(j\omega_2 a_1) \cos(\omega_c \tau - \theta_1(t) + \theta_1(t+\tau)) \\ & \sum_{m_2=0}^{\infty} \epsilon_{m_2} I_{m_2}(j\omega_1 a_2) I_{m_2}(j\omega_2 a_2) \cos(\omega_c \tau - \theta_2(t) + \theta_2(t+\tau)) \\ & \vdots \\ & \sum_{m_M=0}^{\infty} \epsilon_{m_M} I_{m_M}(j\omega_1 a_M) I_{m_M}(j\omega_2 a_M) \cos(\omega_c \tau - \theta_M(t) + \theta_M(t+\tau)) \quad (A.27) \end{aligned}$$

The summations can be grouped together so that $\psi_s(\omega_1, \omega_2, \tau)$ can be written as

$$\begin{aligned} \psi_s(\omega_1, \omega_2, \tau) = & \sum_{m_1=0}^{\infty} \sum_{m_2=0}^{\infty} \dots \sum_{m_M=0}^{\infty} [\epsilon_{m_1} \epsilon_{m_2} \dots \epsilon_{m_M} \prod_{i=1}^M [I_{m_i}(j\omega_1 a_i) I_{m_i}(j\omega_2 a_i)]] \\ & \times \prod_{i=1}^M \cos(\omega_c \tau - \theta_i(t) + \theta_i(t+\tau)) \quad (A.28) \end{aligned}$$

From Eq (A.16), second characteristic function of the noise is written again as

$$\psi_n(\omega_1, \omega_2, \tau) = e^{-\frac{(\omega_1^2 + \omega_2^2) R_n(0)}{2}} \sum_{k=0}^{\infty} \frac{(-1)^k R_n^k(\tau) \omega_1^k \omega_2^k}{k!} \quad (A.29)$$

By combining Eqs (A.4), (A.28), and (A.29), the output autocorrelation of the nonlinear device can now be written as

$$R_y(\tau) = \frac{1}{2\pi} \int_{-\infty}^{\infty} \int_{-\infty}^{\infty} G(\omega_1) G(\omega_2) \sum_{k=0}^{\infty} \frac{(-1)^k R_n^k(\tau)}{k!} \sum_{m_1=0}^{\infty} \sum_{m_2=0}^{\infty} \dots \sum_{m_M=0}^{\infty} \epsilon_{m_1} \epsilon_{m_2} \dots \epsilon_{m_M} \times \omega_1^k e^{-\frac{R_n(0)\omega_1^2}{2}} \omega_2^k e^{-\frac{R_n(0)\omega_2^2}{2}} \prod_{i=1}^M [I_{m_i}(\omega_1 a_i) I_{m_i}(\omega_2 a_i)] \times \prod_{i=1}^M \cos(\omega_c \tau - \theta_i(t) + \theta_i(t+\tau)) \quad (A.30)$$

The autocorrelation can be simplified to form

$$R_y(\tau) = \sum_{k=0}^{\infty} \frac{(-1)^k (R_n^k(\tau)/k!)}{\sum_{m_1=0}^{\infty} \sum_{m_2=0}^{\infty} \dots \sum_{m_M=0}^{\infty} [\epsilon_{m_1} \epsilon_{m_2} \dots \epsilon_{m_M} h_k^2(m_1, m_2, \dots, m_M)]} \times \prod_{i=1}^M \cos(\omega_c \tau - \theta_i(t) + \theta_i(t+\tau)) \quad (A.31)$$

where

$$h_k(m_1, m_2, \dots, m_M) = \frac{1}{2\pi} \int_{-\infty}^{\infty} G(\omega) \omega^k e^{-\frac{R_n(0)\omega^2}{2}} \prod_{i=1}^M I_{m_i}(\omega a_i) d\omega \quad (A.32)$$

which can also be written as

$$h_k(m_1, m_2, \dots, m_M) = (1/2\pi) \int_{-\infty}^{\infty} G(\omega) \omega^k e^{j n (0) \omega^2 / 2 (m_1 + m_2 + \dots + m_M)}$$

$$\times \prod_{i=1}^M I_{m_i}(\omega a_i) d\omega \quad (A.33)$$

From Eq (A.31) the output signal power for the i th signal can now be found as is done in chapter three for a hard limiter.

AD-A151 710

MARGIN LEVELING ALGORITHM FOR FULLY SATURATED SATELLITE 2/2

TRANSPONDER WITH (U) AIR FORCE INST OF TECH

WRIGHT-PATTERSON AFB OH SCHOOL OF ENGI.. E J PUTT

UNCLASSIFIED

DEC 84 AFIT/GE/ENG/84D-52

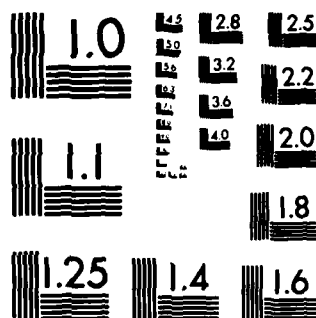
F/G 17/2

NL

END

FILED

DEC



MICROCOPY RESOLUTION TEST CHART
NATIONAL BUREAU OF STANDARDS-1963-A

Bibliography

1. Gagliardi, Robert M. Satellite Communications, Toronto: Wadsworth ,Inc., 1984.
2. Middleton, David. An Introduction to Statistical Communication Theory. New York: McGraw - Hill Book Company, 1960.
3. Bell, W. W. Special Functions for Scientists and Engineers. London: D. Van Nostrand Company, LTD, 1968.
4. Papoulis, Athanasios. Probability, Random Variables and Stochastic Processes. New York: McGraw - Hill Book Company 1965.
5. Shaft, Paul D. "Limiting of Several Signals and Its Effect on Communication System Performance," IEEE Transaction on Communication Theory, 13: 504-512 (Dec 1965).
6. Selby, Samuel M. Standard Mathematical Tables. Cleveland: The Chemical Rubber Co., 1968.
7. IMSL Library Reference Manual, Edition 9, Volume 1-4. IMSL, Inc. June 1982.

VITA

Lieutenant Edward J. Putt was born on 12 October 1959 in Allegany, New York. Upon graduation from high school he enlisted in the USAF in June 1977. After completion of basic training and technical school in October 1977, he served as a F-15 weapons mechanic at the 36 TFW, Bitburg AFB, Germany. In January 1979, he attended the Ohio State University through the AFROTC College Scholarship Program and received a Bachelor of Science in Electrical Engineering in January 1983. Upon graduation he received a commission in the USAF through ROTC and entered the School of Engineering at the Air Force Institute of Technology, Wright Patterson AFB, Ohio.

Permanent address: Box 74

Birch Run Road

Allegany, New York 14706

UNCLASSIFIED

SECURITY CLASSIFICATION OF THIS PAGE

REPORT DOCUMENTATION PAGE

1a. REPORT SECURITY CLASSIFICATION UNCLASSIFIED		1b. RESTRICTIVE MARKINGS	
2a. SECURITY CLASSIFICATION AUTHORITY		3. DISTRIBUTION/AVAILABILITY OF REPORT Approved for public release; distribution unlimited.	
2b. DECLASSIFICATION/DOWNGRADING SCHEDULE		5. MONITORING ORGANIZATION REPORT NUMBER(S)	
4. PERFORMING ORGANIZATION REPORT NUMBER(S) AFIT/GE/ENG/84D-52		7a. NAME OF MONITORING ORGANIZATION	
6a. NAME OF PERFORMING ORGANIZATION School of Engineering	6b. OFFICE SYMBOL (If applicable) AFIT/ENG	7b. ADDRESS (City, State and ZIP Code)	
6c. ADDRESS (City, State and ZIP Code) Air Force Institute of Technology Wright-Patterson AFB, Ohio 45433		9. PROCUREMENT INSTRUMENT IDENTIFICATION NUMBER	
8a. NAME OF FUNDING/SPONSORING ORGANIZATION See box 19	8b. OFFICE SYMBOL (If applicable)	10. SOURCE OF FUNDING NOS.	
8c. ADDRESS (City, State and ZIP Code) 1860 Wiehle Avenue Reston, VA 22090		PROGRAM ELEMENT NO.	PROJECT NO.
11. TITLE (Include Security Classification) See box 19		TASK NO.	WORK UNIT NO.
12. PERSONAL AUTHOR(S) Edward J. Putt, 2Lt, USAF			
13a. TYPE OF REPORT MS Thesis	13b. TIME COVERED FROM _____ TO _____	14. DATE OF REPORT (Yr., Mo., Day) 1984 December	15. PAGE COUNT 99
16. SUPPLEMENTARY NOTATION (See box 19 VIII)			
17. COSATI CODES		18. SUBJECT TERMS (Continue on reverse if necessary and identify by block number)	
FIELD	GROUP	SUB. GR.	
17	02		
09	03		
19. ABSTRACT (Continue on reverse if necessary and identify by block number)			
8a. Defense Communications Engineering Center			
11. Title: Margin Leveling Algorithm for Fully Saturated Satellite Transponder with CDMA Signalling			
Thesis Advisor: Kenneth G. Castor, Maj, USAF			
Approved for public release. LAW AFR 190-17. LTJEN E. WOLATON Deputy for Research Air Force Institute of Technology Wright-Patterson AFB, Ohio 45433-6151 Development			
20. DISTRIBUTION/AVAILABILITY OF ABSTRACT UNCLASSIFIED/UNLIMITED <input checked="" type="checkbox"/> SAME AS RPT. <input type="checkbox"/> DTIC USERS <input type="checkbox"/>		21. ABSTRACT SECURITY CLASSIFICATION UNCLASSIFIED	
22a. NAME OF RESPONSIBLE INDIVIDUAL Kenneth G. Castor, Maj, USAF	22b. TELEPHONE NUMBER (Include Area Code) 513-429-4153	22c. OFFICE SYMBOL AFIT/ENG	

19.

Abstract

For satellite communications in a noninterfering environment, a specific downlink carrier-to-noise ratio is needed to achieve a desired bit error rate. In an interfering environment, an additional carrier-to-noise ratio or margin is needed to overcome the interfering effects. A situation may arise where the desired margins cannot be achieved due to limited uplink and satellite transmit power. If this is the case, margin leveling should occur in order to decrease the desired margins in a specific manner until all margins are achieved.

The goal of this thesis is to develop a margin leveling algorithm under specific constraints. The satellite under study is assumed to be operating with the TWT in full saturation. The signalling scheme used is direct sequence code division multiple access communications.

Two methods of margin leveling are created. The first being the margin leveling of only the links in which the desired margins are not achieved. The second being the margin leveling of all links whether the desired margins are achieved or not. In the latter case, all links are leveled by an equal amount.

Due to the specific satellite model used, the cascade of two bandpass limiters, the amount of computer time needed to perform margin leveling is quite high. It is found that the computer time needed to perform margin leveling increases proportionally to the square of the number of links accessing the satellite.

Given the proper amount of computer time, the results of the margin leveling algorithm were as expected. For either case of margin leveling, the algorithm produced leveled margins with the difference between the desired and the leveled margins being a minimum.

END

FILMED

4-85

DTIC